

## **Vegetation/ecosystem modeling and analysis project: Comparing biogeography and biogeochemistry models in a continental-scale study of terrestrial ecosystem responses to climate change and CO<sub>2</sub> doubling**

VEMAP Members<sup>1</sup>

**Abstract.** We compare the simulations of three biogeography models (BIOME2, Dynamic Global Phytogeography Model (DOLY), and Mapped Atmosphere-Plant Soil System (MAPSS)) and three biogeochemistry models (BIOME-BGC (*BioGeochemistry Cycles*), CENTURY, and Terrestrial Ecosystem Model (TEM)) for the conterminous United States under contemporary conditions of atmospheric CO<sub>2</sub> and climate. We also compare the simulations of these models under doubled CO<sub>2</sub> and a range of climate scenarios. For contemporary conditions, the biogeography models successfully simulate the geographic distribution of major vegetation types and have similar estimates of area for forests (42 to 46% of the conterminous United States), grasslands (17 to 27%), savannas (15 to 25%), and shrublands (14 to 18%). The biogeochemistry models estimate similar continental-scale net primary production (NPP; 3125 to 3772 × 10<sup>12</sup> gC yr<sup>-1</sup>) and total carbon storage (108 to 118 × 10<sup>15</sup> gC) for contemporary conditions. Among the scenarios of doubled CO<sub>2</sub> and associated equilibrium climates produced by the three general circulation models (Oregon State University (OSU), Geophysical Fluid Dynamics Laboratory (GFDL), and United Kingdom Meteorological Office (UKMO)), all three biogeography models show both gains and losses of total forest area depending on the scenario (between 38 and 53% of conterminous United States area). The only consistent gains in forest area with all three models (BIOME2, DOLY, and MAPSS) were under the GFDL scenario due to large increases in precipitation. MAPSS lost forest area under UKMO, DOLY under OSU, and BIOME2 under both UKMO and OSU. The variability in forest area estimates occurs because the hydrologic cycles of the biogeography models have different sensitivities to increases in temperature and CO<sub>2</sub>. However, in general, the biogeography models produced broadly similar results when incorporating both climate change and elevated CO<sub>2</sub> concentrations. For these scenarios, the NPP estimated by the biogeochemistry models increases between 2% (BIOME-BGC with UKMO climate) and 35% (TEM with UKMO climate). Changes in total carbon storage range from losses of 33% (BIOME-BGC with UKMO climate) to gains of 16% (TEM with OSU climate). The CENTURY responses of NPP and carbon storage are positive and intermediate to the responses of BIOME-BGC and TEM. The variability in carbon cycle responses occurs because the hydrologic and nitrogen cycles of the biogeochemistry models have different sensitivities to increases in temperature and CO<sub>2</sub>. When the biogeochemistry models are run with the vegetation distributions of the biogeography models, NPP ranges from no response (BIOME-BGC with all three biogeography model vegetations for UKMO climate) to increases of 40% (TEM with MAPSS vegetation for OSU climate). The total carbon storage response ranges from a decrease of 39% (BIOME-BGC with MAPSS vegetation for UKMO climate) to an increase of 32% (TEM with MAPSS vegetation for OSU and GFDL climates). The UKMO responses of BIOME-BGC with MAPSS vegetation are primarily caused by decreases in forested area and temperature-induced water stress. The OSU and GFDL responses of TEM with MAPSS vegetations are primarily caused by forest expansion and temperature-enhanced nitrogen cycling.

<sup>1</sup>J. M. Melillo, The Ecosystems Center, Marine Biological Laboratory, Woods Hole, Massachusetts; J. Borchers, U.S. Department of Agriculture Forest Service, Oregon State University, Corvallis; J. Chaney, U.S. Department of Forest Service, Oregon State University, Corvallis; H. Fisher, University Corporation for Atmospheric Research, Boulder, Colorado; S. Fox, U.S. Department of Agriculture Forest

Service, Raleigh, North Carolina; A. Haxeltine, University of Lund, Lund, Sweden; A. Janetos, National Aeronautics and Space Administration, Washington, D.C.; D. W. Kicklighter, The Ecosystems Center, Marine Biological Laboratory, Woods Hole, Massachusetts; T. G. F. Kittel, University Corporation for Atmospheric Research, Boulder, Colorado; A. D. McGuire, Alaska Cooperative Fish and Wildlife Research Unit, University of Alaska-Fairbanks; R. McKeown, Natural Resources Ecology Laboratory, Colorado State University, Fort Collins; R. Neilson, U.S. Department of Agriculture Forest Service, Oregon State University, Corvallis; R. Nemani, University of Montana, Missoula; D. S. Ojima, Natural Resources Ecology Laboratory, Colorado State University, Fort Collins; T. Painter, Center for Remote Sensing and

Environmental Optics, University of California, Santa Barbara; Y. Pan, The Ecosystems Center, Marine Biological Laboratory, Woods Hole, Massachusetts; W. J. Parton, Natural Resources Ecology Laboratory, Colorado State University, Fort Collins, Colorado; L. Pierce, Department of Biological Sciences, Stanford University, Stanford, California; L. Pitelka, Electric Power Research Institute, Palo Alto, California; C. Prentice, University of Lund, Lund, Sweden; B. Rizzo, Department of Environmental Sciences, University of Virginia, Charlottesville; N. A. Rosenbloom, Department of Geology, Institute of Arctic and Alpine Research, University of Colorado, Boulder; S. Running, University of Montana, Missoula; D. S. Schimel, University Corporation for Atmospheric Research, Boulder, Colorado; S. Sitch, University of Lund, Lund, Sweden; T. Smith, Department of Environmental Sciences, University of Virginia, Charlottesville; I. Woodward, Department of Animal and Plant Sciences, University of Sheffield, Sheffield, England.

## Introduction

The atmospheric concentrations of the major long-lived greenhouse gases continue to increase because of human activity. Changes in greenhouse gas concentrations and aerosols are likely to affect climate through changes in temperature, cloud cover, and precipitation [Intergovernmental Panel on Climate Change (IPCC), 1992; Charlson and Wigley, 1994; Penner *et al.*, 1994]. Changes in land cover and land use may also influence climate at the regional scale [Dirmeyer, 1994; Trenberth *et al.*, 1988; Nobre *et al.*, 1991]. Predictions of the climate system's response to altered forcing are shifting from a simplistic view of global warming to a more complex view involving a range of regional responses, aerosol offsets and large scale feedbacks and interactions. There is considerable concern over the extent to which these changes could affect both natural and human-dominated ecosystems [Melillo *et al.*, 1990; Walker, 1994; Schimel *et al.*, 1994]. Because the response of the climate system to anthropogenic forcing will likely have considerable spatial complexity, a capability to assess spatial variations in ecological response to climate forcing is critical.

On the basis of our understanding of ecological principles, we can expect that changes in climate and atmospheric composition should affect both the structure and function of terrestrial ecosystems. Structural responses include changes in species composition and in a variety of vegetation characteristics such as canopy height and rooting depth. Functional responses include changes in the cycling of carbon, nutrients (e.g., nitrogen, phosphorus, sulfur) and water.

Models of how ecosystem structure (biogeography models) and function (biogeochemistry models) might respond to climate change exist, but generally have been developed independently. In recent years, both types of models have been exercised for large regions or even the entire globe using various climate change scenarios [Melillo *et al.*, 1993; Neilson and Marks, 1995; Prentice *et al.*, 1992; Prentice and Fung, 1990; Schimel *et al.*, 1994]. Any serious attempt to assess how global change will affect a particular region must include both aspects of ecological response. While it may not yet be possible to formally link specific models so that the biogeography and biogeochemistry are truly interactive, it is both possible and desirable to begin to combine the two aspects of ecosystem response for sensitivity studies.

In such an exercise it is important to recognize that a diversity of both biogeography and biogeochemistry models exist. Our understanding of the controls of ecosystem structure and function

currently is not sufficient to allow the identification of the "best" models or to accept as correct their predictions. Thus in any effort to provide more realistic simulations of ecological response, it is important to employ several models of each type and to compare models that attempt to simulate the same types of response. In this paper we present an overview of the results of the Vegetation/Ecosystem Modeling and Analysis Project (VEMAP), an international collaborative exercise involving investigators from thirteen institutions.

## Approach

### Overview

We compare the simulations of three biogeography models (BIOME2, DOLY, and MAPSS) and three biogeochemistry models (BIOME-BGC, CENTURY, and TEM) for the conterminous United States under contemporary conditions of atmospheric CO<sub>2</sub> and climate. We also compare the simulations of these models under doubled CO<sub>2</sub> and a range of climate scenarios. In addition, we simulate a coupled response by using the biogeography model outputs as inputs to the biogeochemistry models.

It is often difficult to identify the source of inconsistencies in outputs from model intercomparisons. Differences in model outputs may arise from differences in conceptualization of the problem, implementation at different spatial or temporal scales, or use of different input data sets. Contrasts in model conceptualizations can occur either with the use of different algorithms or parameter values. In order to examine how different algorithms or parameter values of identical algorithms influence change, we attempt to minimize the other sources of variation by using a common input database and a common spatial format. In this section, we (1) describe the models used in this project, (2) present the input database, and (3) discuss the project's experimental design.

### Model Descriptions

**Biogeography Models.** The biogeography models predict the dominance of various plant life forms in different environments, based on two types of boundary conditions: ecophysiological constraints and resource limitations. Ecophysiological constraints determine the distribution of major categories of woody plants and are implemented in the models through the calculation of bioclimatic variables such as growing degree days and minimum winter temperatures. Resource (e.g., water, light) limitations determine major structural characteristics of vegetation, including leaf area. The differential responses of plant life forms to resource limitations determine aspects of vegetation composition such as the competitive balance of trees and grasses. To account for the effects of resource limitations, the models simulate potential evapotranspiration (PET), actual evapotranspiration (ET), and in two of the models, net primary production (NPP) (Tables 1 and 2). In the VEMAP activity we have used three biogeography models: BIOME2 [Haxeltine *et*

**Table 1.** Vegetation Discrimination Criteria in the Biogeography Models

Vegetation Definition	BIOME2	DOLY	MAPSS
Evergreen/deciduous	cold tolerance, chilling, annual C balance, drought	cold tolerance, low temperature growth limit, drought	cold tolerance, summer drought, summer C balance
Needleleaf/broadleaf	cold tolerance, GDD	cold tolerance, GDD	cold tolerance, summer drought, GDD
Tree/shrub	precipitation seasonality	NPP, LAI, moisture balance	LAI
Woody/non-woody	annual C balance, FPC	moisture balance, NPP, LAI	understory light
C <sub>3</sub> /C <sub>4</sub>	temperature	growing season temperature	soil temperature
Continental/maritime	winter temperature	GDD, winter minimum temperature	winter-summer temperature difference

GDD is growing degree days; LAI is leaf area index; NPP is net primary production; FPC is foliar projected cover.

*al.*, 1995], DOLY [Woodward and Smith, 1994a; Woodward *et al.*, 1995], and MAPSS [Neilson, 1995].

**BIOME2:** In BIOME2, ecophysiological constraints, which are based largely on the BIOME model of Prentice *et al.* [1992], are applied first to select which plant types are potentially present at a particular location. Starting from this initial set, the model then identifies the quantitative combination of plant types that maximizes whole ecosystem NPP.

Gross primary production (GPP) is calculated on a monthly time step as a linear function of absorbed photosynthetically active radiation based on a modification of the Farquhar photosynthesis equation [Haxeltine and Prentice, 1995]. The GPP is reduced by drought stress and low temperatures. Respiration costs are currently estimated simply as 50% of the non-water-limited GPP. The model simulates maximum sustainable foliar projected cover (FPC) as the FPC that produces maximum NPP. Through the effect of drought stress on NPP, the model simulates changes in FPC along moisture gradients.

A two-layer hydrology model with a daily time step allows simulation of the competitive balance between grass and woody vegetation, including the effects of soil texture, based on differences in rooting depth. The prescribed CO<sub>2</sub> concentration has a direct effect on GPP through the photosynthesis algorithm, and affects the competitive balance between C<sub>3</sub> and C<sub>4</sub> plants.

The water balance calculation is based upon equilibrium evapotranspiration theory [Jarvis and McNaughton, 1986] which suggests that the large-scale PET is primarily determined by the energy supply for evaporation, and is progressively lowered as soil water content declines. There is no direct effect of CO<sub>2</sub> on the water balance in the model.

**DOLY:** The DOLY model simulates photosynthesis and ET at a daily time step, using the Farquhar *et al.* [1980] and Penman-Monteith [Monteith, 1981] models, respectively. Maximum assimilation and respiration rates are affected by both temperature and nitrogen. Total nitrogen uptake is derived from soil carbon and nitrogen contents and depends on temperature and moisture [Woodward and Smith, 1994b]. The influences of CO<sub>2</sub> concentration on NPP and ET are modeled explicitly. The maximum sustainable leaf area index (LAI) for a location is estimated from long-term average annual carbon and hydrologic budgets, as the highest LAI that is consistent with maintaining the soil water balance.

In the DOLY model an empirical statistical procedure, implemented after the biogeochemical process calculations, is used to derive the vegetation. This procedure takes account of both ecophysiological constraints and resource limitation effects, based on their observed outcome in a range of climates today. Estimates of NPP, LAI, ET, and PET are combined with

**Table 2.** Treatments of Biogeochemical Process in the Biogeography Models

State Variables	BIOME2	DOLY	MAPSS
PET/ET	equilibrium	Penman-Monteith	aerodynamic [Marks, 1990]
Stomatal conductance	implicit via soil water content	soil water content, VPD, photosynthesis., soil nitrogen	soil water potential, VPD
Productivity index	NPP(Farquhar-Collatz)	NPP(Farquhar, N uptake)	leaf area duration
LAI/FPC	water balance, temperature	water balance, light, nitrogen	water balance, temperature
Number of soil water layers	two layer, saturated and unsaturated percolation	one layer	three layer, saturated and unsaturated percolation

PET is potential evapotranspiration; ET is evapotranspiration; VPD is vapor pressure deficit; NPP is net primary production.; LAI is leaf area index; FPC is foliar projected cover.

bioclimatic variables (absolute minimum temperature, growing degree days (base temperature 0° C), annual precipitation) and a previously defined vegetation classification to develop a biogeography model using multiple discriminant function analysis, as in work by *Rizzo and Wiken [1992]*.

**MAPSS:** The MAPSS model begins with the application of ecophysiological constraints to determine which plant types can potentially occur at a given location. A two-layer hydrology module (including gravitational drainage) with a monthly time step then allows simulation of leaf phenology, LAI and the competitive balance between grass and woody vegetation. A productivity index is derived based on leaf area duration and ET. This index is used to assist in the determination of leaf form, phenology, and vegetation type, on the principle that any successful plant strategy must be able to achieve a positive NPP during its growing season.

The LAI of the woody layer provides a light-limitation to grass LAI. Stomatal conductance is explicitly included in the water balance calculation, and water competition occurs between the woody and grass life-forms through different canopy conductance characteristics as well as rooting depths. The direct effect of CO<sub>2</sub> on the water balance is simulated by reducing maximum stomatal conductance. The MAPSS model is calibrated against observed monthly runoff, and has been validated against global runoff [*Neilson and Marks, 1995*]. A simple fire model is incorporated to limit shrubs in areas such as the Great Plains [*Neilson, 1995*].

The forest-grassland ecotone is reproduced by assuming that closed forest depends on a predictable supply of winter precipitation for deep soil recharge [*Neilson et al., 1992*]. An index is used that decrements the woody LAI as the summer dependency increases.

**Comparison of biogeography models:** The three vegetation biogeography models use similar thermal controls on plant life form distribution (Table 1). In addition, they all calculate a physically based water balance to control water-limited vegetation distribution (Table 2). The MAPSS and BIOME2 models partition soil water between upper (grass and woody plant) and lower (woody plant) rooting zones. Leaf area, (LAI in MAPSS and DOLY, FPC in BIOME2) is treated as a key determinant of vegetation structure. Transpiration is linked to leaf area. In water-limited environments, leaf area is assumed to increase to a level above which deleterious water deficits would result. Additional energetic constraints (and in DOLY, a nitrogen availability constraint) on leaf area are imposed in cold environments. Thus there is a common conceptual core to all three models' treatments of both thermal responses and hydrological interactions.

Important differences among models lie in their representations of potential evapotranspiration and direct CO<sub>2</sub> effects. Key abiotic controls on potential evapotranspiration are available energy (a function of net radiation and temperature) and the vapor pressure deficit (VPD) above the canopy. These controls are a complex function of canopy properties, planetary boundary layer dynamics and spatial scale [*Jarvis and McNaughton, 1986*]. The three models make different simplifying assumptions, which result in different sensitivities to temperature and canopy characteristics. In BIOME2, potential evapotranspiration is assumed to be fully determined by the available energy supply, which implies no sensitivity to

temperature-induced changes in vapor pressure deficit, or to canopy properties. The MAPSS model uses an aerodynamic approach [*Marks, 1990*] which allows sensitivity to canopy characteristics (stomatal conductance, LAI, and roughness length), and a much greater sensitivity to temperature-induced changes in VPD. The DOLY model uses the Penman-Monteith approach, which is intermediate.

The differences among the models' treatments of evapotranspiration also lead to differences in CO<sub>2</sub> response. In MAPSS, increasing CO<sub>2</sub> reduces stomatal conductance and therefore also reduces transpiration, allowing a greater sustainable LAI. The strong sensitivity of LAI to CO<sub>2</sub> in MAPSS offsets its sensitivity to temperature-induced changes in VPD. However, there is no representation of the effects of CO<sub>2</sub> on carbon balance, or on the competition of C<sub>3</sub> and C<sub>4</sub> plants. In BIOME2, CO<sub>2</sub> affects this competition (via the NPP calculation), but there is no representation of the effects of CO<sub>2</sub> on transpiration or LAI. In DOLY, increasing CO<sub>2</sub> both reduces stomatal conductance (allowing greater LAI where water is limiting) and increases NPP, but does not affect the competition of C<sub>3</sub> and C<sub>4</sub> plants.

**Biogeochemistry Models.** The biogeochemistry models simulate the cycles of carbon, nutrients (e.g., nitrogen), and water in terrestrial ecosystems which are parameterized according to life-form type (Table 3). The models consider how these cycles are influenced by environmental conditions, including temperature, precipitation, solar radiation, soil texture, and atmospheric CO<sub>2</sub> concentration (Table 4). These environmental variables are inputs to general algorithms that describe plant and soil processes such as carbon capture by plants with photosynthesis, decomposition, soil nitrogen transformations mediated by microorganisms, and water flux between the land and the atmosphere in the processes of evaporation and transpiration. Common outputs from biogeochemistry models are estimates of net primary productivity, net nitrogen mineralization, evapotranspiration fluxes (e.g., PET, ET), and the storage of carbon and nitrogen in vegetation and soil. In the VEMAP activity we have used three biogeochemistry models: BIOME-BGC, [*Hunt and Running, 1992; Running and Hunt, 1993*], CENTURY [*Parton et al., 1987; Parton et al., 1988; Parton et al., 1993*], and the Terrestrial Ecosystem Model [TEM, *Raich et al., 1991; McGuire et al., 1992; Melillo et al., 1993*]. The similarities and differences among the models are summarized in Table 5.

**BIOME-BGC:** The BIOME-BGC (*BioGeochemical Cycles*) model is a multibiome generalization of FOREST-BGC, a model originally developed to simulate a forest stand development through a life cycle [*Running and Coughlan, 1988; Running and Gower, 1991*]. The model requires daily climate data and the definition of several key climate, vegetation, and site conditions (Table 4) to estimate fluxes of carbon, nitrogen, and water through ecosystems. Allometric relationships are used to initialize plant and soil carbon (C) and nitrogen (N) pools based on the leaf pools of these elements [*Vitousek et al., 1988*]. Components of BIOME-BGC have previously undergone testing and validation, including the carbon dynamics [*McLeod and Running, 1988; Korol et al., 1991; Hunt et al., 1991; Pierce, 1993; Running, 1994*] and the hydrology [*Knight et al., 1985; Nemani and Running, 1989; White and Running, 1995*].

**CENTURY:** The CENTURY model (Version 4) simulates

**Table 3.** Basic Life-forms Used in the Parameterization of the Biogeochemistry Models for Different Vegetation Types

Vegetation Description	BIOME-BGC	CENTURY	TEM
Tundra	C <sub>3</sub> grassland	tundra	alpine tundra
Boreal coniferous forest	coniferous forest	subalpine fir: 100yr burn	boreal coniferous forest
Temperate maritime coniferous forest	coniferous forest	western pine: 500yr burn	maritime temperate coniferous forest
Temperate continental coniferous forest	coniferous forest	western pine: 100yr burn	continental temperate coniferous forest
Cool temperate mixed forest	50% coniferous forest, 50% deciduous forest	northeast-temperate mixed: 500yr burn	50% continental temperate coniferous forest, 50% temperate deciduous forest
Warm temperate/Subtropical mixed forest	50% coniferous forest, 50% deciduous forest	southeast mixed: 200yr burn/blowdown	33% continental temperate coniferous forest, 33% temperate deciduous forest, 34% temperate broadleaved evergreen forest
Temperate deciduous forest	deciduous forest	northeast deciduous: 500yr burn	temperate deciduous forest
Tropical deciduous forest	deciduous forest	tropical deciduous: 500yr burn	tropical forest
Tropical evergreen forest	broadleaved evergreen forest	tropical deciduous: 500yr burn	tropical forest
Temperate mixed xeromorphic woodland	50% coniferous forest, 50% deciduous forest	southern mixed hardwood/C <sub>3</sub> grass: 30yr forest burn/4yr grass burn, annual grazing	xeromorphic woodland
Temperate conifer xeromorphic woodland	coniferous forest	western pine/ 50% C <sub>3</sub> - 50% C <sub>4</sub> grass mix: 30yr forest burn/ 4yr grass burn, annual grazing	xeromorphic woodland
Tropical thorn woodland	shrubland	southern mixed hardwood/C <sub>4</sub> grass: 100yr forest burn/3yr grass burn, annual grazing	xeromorphic woodland
Temperate deciduous savanna	20% deciduous forest, 80% C <sub>4</sub> grassland	southern mixed hardwood/50% C <sub>3</sub> - 50% C <sub>4</sub> grass mix: 30yr forest burn/4yr grass burn, annual grazing	50% temperate deciduous forest, 50% grassland
Warm temperate/Subtropical mixed savanna	20% deciduous forest, 80% C <sub>4</sub> grassland	southern mixed hardwood/50% C <sub>3</sub> - 50% C <sub>4</sub> grass mix: 30yr forest burn/4yr grass burn, annual grazing	17% continental temperate coniferous forest, 16% temperate deciduous forest, 50% grassland, 17% temperate broadleaved evergreen forest
Temperate conifer savanna	20% coniferous forest, 80% C <sub>3</sub> grassland	western pine/50% C <sub>3</sub> - 50% C <sub>4</sub> grass mix: 30yr forest burn/4yr grass burn, annual grazing	50% continental temperate coniferous forest, 50% grassland
Tropical deciduous savanna	20% deciduous forest, 80% C <sub>4</sub> grassland	southern mixed hardwood/C <sub>4</sub> grass: 30yr forest burn/4yr grass burn, annual grazing	50% tropical forest, 50% grassland
C <sub>3</sub> grasslands	C <sub>3</sub> grassland	C <sub>3</sub> grass: annual grazing	grassland
C <sub>4</sub> grasslands	C <sub>4</sub> grassland	C <sub>4</sub> grass: 3yr grass burn, annual grazing	grassland
Mediterranean shrubland	shrubland	chaparral: 30yr shrub burn	xeromorphic woodland
Temperate arid shrubland	shrubland	sage/75% C <sub>3</sub> - 25% C <sub>4</sub> grass: 30yr shrub burn/4yr grass burn	shrubland
Subtropical arid shrubland	shrubland	creosote/50% C <sub>3</sub> - 50% C <sub>4</sub> grass: 30yr shrub burn/4yr grass burn	shrubland

**Table 4.** Input Requirements of the Biogeography and Biogeochemistry Models for the VEMAP Simulations

Input Variable	Biogeography Models			Biogeochemistry Models		
	BIOME2	DOLY	MAPSS	BIOME-BGC	CENTURY	TEM
Surface climate						
Air temperature						
Mean	M	D	M			M
Minimum		D,A		D	M	
Maximum		D		D	M	
Precipitation	M	D	M	D	M	M
Humidity <sup>a</sup>		D(RH)	M(VP)	D(RH)		
Solar radiation <sup>b</sup>	M(%S)	D(I)		D(SR)		M(%C)
Wind speed		M <sup>c</sup>	M			
Vegetation type				X	X	X
Soil						
Texture <sup>d</sup>	X(CAT)	X(%T)	X(%T,R,O)		X(%T)	X(%T)
Depth		X		X	X	
Water holding capacity		X		X		
Soil C, N		X				
Location						
Elevation				X	X	X
Latitude	X			X	X	X

Required variables are indicated with an 'X', except for climate variables where models required daily (D) or monthly (M) inputs and/or absolute value over record (A).

<sup>a</sup> Humidity variables were average daytime relative humidity (RH) or vapor pressure (VP).

<sup>b</sup> Solar radiation inputs were: total incident solar radiation (SR), daily mean irradiance (I), percent cloudiness (%C), or percent possible sunshine hours (%S).

<sup>c</sup> DOLY can use daily wind speed, but was implemented with monthly inputs for this study.

<sup>d</sup> Texture was input either as %sand, silt, and clay (%T) or as categorical soil type (CAT). Additional textural inputs were rock fraction (R) and organic matter content (O).

the C, N, P, and S dynamics of grasslands, forests, and savannas [Parton *et al.*, 1987, 1993; Metherell, 1992]. For VEMAP only C and N dynamics are included. The model uses monthly temperature and precipitation data (Table 4) as well as atmospheric CO<sub>2</sub> and N inputs to estimate monthly stocks and fluxes of carbon and nitrogen in ecosystems. The CENTURY model also includes a water budget submodel which calculates monthly evaporation, transpiration, water content of the soil layers, snow water content, and saturated flow of water between soil layers. The CENTURY model incorporates algorithms that describe the impact of fire, grazing, and storm disturbances (Table 3) on ecosystem processes [Ojima *et al.*, 1990; Sanford *et al.*, 1991; Holland *et al.*, 1992; Metherell, 1992].

**TEM:** The Terrestrial Ecosystem Model (TEM Version 4) describes carbon and nitrogen dynamics of plants and soils for nonwetland ecosystems of the globe [McGuire *et al.*, 1995a]. The TEM requires monthly climatic data (Table 4) and soil and vegetation-specific parameters to estimate monthly carbon and nitrogen fluxes and pool sizes. Hydrological inputs for TEM are

determined by a water balance model [Vörösmarty *et al.*, 1989] that uses the same climatic data and soil-specific parameters as used in TEM. Estimates of net primary production and carbon storage by TEM have been evaluated in previous applications of the model at both regional and global scales [Raich *et al.*, 1991; McGuire *et al.*, 1992, 1993, 1995b; Melillo *et al.*, 1993, 1995].

**Comparison of biogeochemistry models:** All three biogeochemistry models include submodels of the carbon, nitrogen, and water cycles, and simulate the interactions among these cycles. Both CENTURY and TEM operate on a monthly time step and BIOME-BGC operates on a daily time step. The models differ in terms of the emphasis placed on particular biogeochemical cycles and the feedback of these cycles on ecosystem dynamics. The BIOME-BGC model relies primarily on the hydrologic cycle and the control of water availability on C uptake and storage. Both CENTURY and TEM rely primarily on the nitrogen cycle and the control of nitrogen availability on C uptake and storage. Below we review several of the differences among the models including their representation of various

**Table 5.** Comparison of Biogeochemical Processes and Compartments Among the Biogeochemistry Models

Process	BIOME-BGC	CENTURY	TEM
PET/ET	Penman-Monteith	modified Penman-Monteith	<i>Jensen-Haise</i> [1963]
Number of soil water layers	1	5-7	1
Carbon uptake by vegetation	Farquhar	multiple limitation NPP	multiple limitation GPP
LAI	water balance <sup>a</sup> , N availability and gross photosynthesis	leaf biomass, relative carbon allocation to different vegetation pools	not explicitly calculated
$C_i = f(C_a)$	yes	not applicable	yes
Stomatal conductance = $f(C_a)$	yes	yes	no
Vegetation C/N = $f(C_a)$	yes	yes	no
Plant respiration $Q_{10}$	2.0	2.0	1.5 - 2.5
Decomposition $Q_{10}$	2.4	~2.0	2.0
Number of vegetation carbon pools	4	8	1
Number of litter/soil carbon pools	3	13	1
Nitrogen uptake by vegetation	annual	monthly	monthly
NMIN	C/N ratio controlled	C/N ratio controlled, $f$ (moisture, temperature)	mineralization/ immobilization dynamics
Number of vegetation nitrogen pools	4	8	2
Number of litter/soil nitrogen pools	3	15	2
Equilibrium	carbon pools specified so that NEP = 0 after 1 year	simulation with repeated disturbance for 2000 years	dynamic simulation (10 to 3000 years) until carbon and nitrogen pools come into balance (e.g., NEP = 0, NMIN = NUPTAKE, N input = N lost)
Temporal scale	daily/annual	monthly	monthly

PET is potential evapotranspiration; ET is evapotranspiration; LAI is leaf area index;  $C_a$  is atmospheric  $CO_2$  concentration;  $C_i$  is the internal  $CO_2$  concentration within a "leaf"; NPP is net primary production; GPP is gross primary production; NMIN is net nitrogen mineralization; NEP is net ecosystem production; and NUPTAKE is nitrogen uptake by vegetation.

<sup>a</sup> for the VEMAP activity, LAI is a function of only water balance

ecosystem components and the algorithms used to describe ecosystem processes.

**Carbon and nitrogen pools:** Although all the models estimate the C and N pools in vegetation and soil, these pools are simulated with varying degrees of complexity. For example, TEM represents vegetation carbon with only one compartment; BIOME-BGC has four; and CENTURY has eight (Table 5). To compare model estimates in the VEMAP activity, a total vegetation carbon (VEGC) estimate (above and belowground) is determined for each model by summing the component pools. Similarly, a total soil carbon (SOILC) estimate is determined by summing all litter and soil organic matter pools. Total carbon estimates are then calculated by summing total vegetation carbon and total soil carbon.

**Net primary productivity (NPP):** Although all the models estimate NPP by subtracting plant respiration from a gross carbon uptake rate, these estimates are derived in different ways (Table 5). The BIOME-BGC model estimates NPP and plant respiration by dividing total canopy photosynthesis in half. Total canopy photosynthesis estimates are based on the models of *Farquhar et al.* [1980] and *Leuning* [1990] using estimates of

leaf conductance, leaf nitrogen, intercellular  $CO_2$  concentration, air temperature, incident solar radiation, and leaf area index [*Field and Mooney*, 1986; *Woodrow and Berry*, 1988; *Rastetter et al.*, 1992].

In CENTURY, maximum plant production is controlled by soil temperature, available water, LAI, and stand age. A temperature-production function is specified according to plant functional types, such as  $C_3$  cool season plants or  $C_4$  warm season plants. Production is further modified by the current amount of aboveground plant material (i.e., self-shading), atmospheric  $CO_2$  concentrations, and available soil N. To simulate savanna and shrubland ecosystems, grass and forest model components compete for water, light, and nutrients in a prescribed manner.

In TEM, NPP is the difference between carbon captured from the atmosphere as gross primary production (GPP) and carbon respired to the atmosphere by the vegetation. Gross primary production is initially calculated in TEM as a function of light availability, air temperature, atmospheric carbon dioxide concentration, and moisture availability. If nitrogen supply, which is the sum of nitrogen uptake and labile nitrogen in the

vegetation, cannot meet the stoichiometric C:N ratio of biomass production, then GPP is reduced to meet the C:N constraint. In the case where nitrogen supply does not limit biomass production, nitrogen uptake is reduced so that nitrogen supply meets the C:N constraint of biomass production. In this way, the carbon-nitrogen status of the vegetation causes the model to allocate more effort toward either carbon or nitrogen uptake [McGuire *et al.*, 1992, 1993]. Plant respiration is a function of the mass of vegetation carbon and air temperature.

**Response to elevated CO<sub>2</sub>:** To simulate the effects of doubling atmospheric CO<sub>2</sub>, both BIOME-BGC and CENTURY prescribe changes in the nitrogen content of vegetation. Photosynthesis in BIOME-BGC is constrained by reducing leaf nitrogen concentration by 20%. In CENTURY, the C:N ratios are increased by 20% on the minimum and maximum ratios for N in shoots of grasses and leaves of trees. In addition, both of the models prescribe changes that affect the hydrologic cycle. The BIOME-BGC model reduces canopy conductance to water vapor by 20% to affect leaf area development. The CENTURY model prescribes a 20% reduction in actual evapotranspiration to influence soil moisture. Indirect effects of increased atmospheric CO<sub>2</sub> concentrations on ecosystem dynamics occur through decomposition feedbacks caused by CO<sub>2</sub>-induced changes in leaf litter quality and soil moisture.

In TEM, elevated CO<sub>2</sub> may affect GPP either directly or indirectly. A direct consequence of elevated atmospheric CO<sub>2</sub> is to increase the intercellular CO<sub>2</sub> concentration within the canopy which potentially increases GPP via a Michaelis-Menton (hyperbolic) relationship. Elevated atmospheric CO<sub>2</sub> may indirectly affect GPP by altering the carbon-nitrogen status of the vegetation to increase effort toward nitrogen uptake; increased effort is generally realized only when GPP is limited more by carbon availability than by nitrogen availability. Potential and actual evapotranspiration are not influenced by CO<sub>2</sub> concentrations.

**Decomposition:** Estimates of decomposition depend on the representation of litter and soil compartments in the various models. In BIOME-BGC, C and N are released from the litter and soil compartments through an algorithm that includes controls by water, temperature, and lignin [Meentemeyer, 1984]. In a similar manner, TEM simulates decomposition as a function of the one soil organic carbon compartment, temperature, and soil moisture. In contrast, the CENTURY model simulates the decomposition of plant residues with a detailed submodel that divides soil organic carbon into three fractions: an active soil fraction (< 10-year turnover time) consisting of live microbes and microbial products; a protected fraction (decadal turnover time) that is more resistant to decomposition as a result of physical or chemical protection; and a fraction that has a very long turnover time (millennial turnover time).

**Equilibrium assumptions:** The modeling groups participating in the VEMAP activity agreed to make model comparisons for mature ecosystems at "equilibrium", but the three model structures dictated that the definition of "equilibrium" be slightly different among them (Table 5). The BIOME-BGC model assumes that equilibrium conditions are reached when net ecosystem production (NEP) is equal to zero (i.e., annual NPP is equal to annual decomposition rates) and NPP is equal to half of total canopy photosynthesis. Similarly, TEM assumes equilibrium conditions are reached when the

annual fluxes of NPP, litterfall carbon, and decomposition are balanced; the annual fluxes of net nitrogen mineralization, litterfall nitrogen, and nitrogen uptake by vegetation are balanced; and nitrogen inputs are equal to nitrogen losses from the ecosystem. In order to bring each simulated ecosystem to equilibrium, CENTURY runs for at least 2000 years for each grid cell with prescribed disturbance regimes for specific ecosystems (Table 3). The disturbances are scheduled so that the model simulation for a grid cell ends at a prescribed stand age.

### Model Input Data

For the VEMAP activity, we developed a model database of current climate, soils, vegetation, and climate change scenarios for the conterminous United States. The database was developed to be compatible with the requirements of the biogeography and biogeochemistry models (Table 4) [Kittel *et al.*, 1995a]. Input requirements varied among models in terms of (1) daily versus monthly climate drivers, (2) number of climate and soil inputs, and (3) different representations of controlling variables such as solar radiation and surface humidity. These differences presented a number of problems in the development of a common input data set. First, daily and monthly data sets had to represent the same mean climate, but the daily set needed to have statistical variability characteristic of daily weather. Second, the requirement for multivariate inputs posed problems of spatial consistency among data layers due to differences in source data resolution, accuracy, and registration [Kittel *et al.*, 1995b]. Finally, the need to generate different representations of the same driving variable led to empirical approximations in cases where relationships between representations are complex.

Key design criteria for the database were that data layers be (1) temporally consistent, with daily and monthly climate sets having the same monthly averages, (2) spatially consistent, with, for example, climate and vegetation reflecting topographic effects, and (3) physically consistent, maintaining relationships among climate variables and among soil properties in soil profiles. The database covers the conterminous United States, using a 0.5° latitude/longitude grid.

**Climate driving variables.** Climate variables required by the suite of models were both daily and monthly fields of minimum and maximum surface air temperature, precipitation, total incident solar radiation, surface air humidity, and surface wind speed (Table 4). The daily set had to have realistic daily variance structure for the daily based models to adequately simulate water balance and ecological dynamics. As a result, daily "normals" (i.e., long-term averages by day-of-year) would not suffice. On the other hand, the monthly time step models generally use long-term monthly climatological data. Therefore the daily climate data set had to have daily variances and covariances characteristic of an actual weather record, but maintain on a monthly basis the same climate as the long-term monthly mean data set. These two requirements were accomplished by (1) stochastically generating daily climates for each grid cell based on temporal statistical properties of nearby weather stations, and (2) constraining the monthly means of the created daily record to match those of the cell's long-term climate.

Spatial and physical consistency among variables were achieved by (1) using monthly mean data developed with spatial

interpolation techniques that account for effects of topography on climate, and (2) using covariance information and empirical relationships between related variables in the generation of daily data. This suite of techniques used to assure temporal, spatial, and physical consistency was implemented in a three-step process.

**Step 1:** Interpolation routines were used to topographically adjust monthly mean temperature, precipitation, and wind speed. To account for the effects of topography on temperature in the gridding of station data, monthly mean minimum and maximum temperatures from 4613 station normals [NCDC, 1992] were first adiabatically adjusted to sea level using algorithms of *Marks and Dozier* [1992]. Adjusted temperatures were then interpolated to the 0.5° grid and adiabatically readjusted to grid elevations.

To create a 0.5° gridded data set of mean monthly precipitation that incorporated orographic effects, we spatially aggregated a 10-km gridded data set developed using Precipitation-Elevation Regressions on Independent Slopes Model (PRISM) [Daly *et al.*, 1994]. The PRISM models precipitation distribution by (1) dividing the terrain into topographic facets of similar aspect, (2) developing precipitation-elevation regressions for each facet by region based on station data, and (3) using these regressions to spatially extrapolate station precipitation to cells that are on similar facets.

Mean monthly wind speeds at 10-m height were derived from *Marks* [1990] based on U.S. Department of Energy seasonal wind averages [Elliott *et al.*, 1986]. Elliott *et al.* [1986] topographically corrected the wind speed means to account for greater speeds over regions with high terrain.

**Step 2:** We used a daily weather generator, a modified version of Weather Generator (WGEN) [Richardson, 1981; Richardson and Wright, 1984] to statistically simulate a year-long series of daily temperature and precipitation, with the constraint that the monthly means of the daily values matched the long-term monthly climatology. Parameterization of WGEN for each cell was based on the daily record of the nearest station drawn from a set of 870 stations [Shea, 1984; Eddy, 1987]. The WGEN created records that realistically represent daily variances and temporal autocorrelations (e.g., persistence of dry and wet days). In addition, WGEN maintained the physical relationship between daily precipitation and temperature by accounting for their daily covariance. For example, days with precipitation had higher minimum and lower maximum temperatures than days with no precipitation.

**Step 3:** We used Climate Simulator (CLIMSIM) (a simplified version of Mountain Microclimate Simulator (MT-CLIM) for flat surfaces) [Running *et al.*, 1987; Glassy and Running, 1994] to estimate daily total incident solar radiation, daily irradiance, and surface humidity based on daily minimum and maximum temperature and precipitation. The objective of this approach was to retain physical relationships between temperature, precipitation, solar radiation, and humidity on a daily basis. Monthly means of solar radiation and humidity were derived from the daily values. The CLIMSIM determines daily solar radiative inputs based on latitude, elevation, diurnal range of temperature, and occurrence of precipitation using algorithms of *Gates* [1981] and *Bristow and Campbell* [1984]. Mean daily irradiance was calculated based on day length. Percent cloudiness and percent potential sunshine hours were estimated from fraction of potential total incident solar radiation using the

regression relationships developed by *Black et al.* [1954] and *Linacre* [1968].

The CLIMSIM empirically estimates daily vapor pressure and average daytime relative humidity by assuming that on a daily basis minimum temperatures reach the dew point. Because this is often not the case in arid regions, we adjusted daily humidity data downward so that vapor pressure monthly means matched the observed monthly climatology developed by *Marks* [1990].

**Soils and vegetation.** An important aspect of the database development was the creation of a common vegetation classification. A common classification simplifies comparison of model results and the coupling of the vegetation redistribution models to the biogeochemistry models. In addition, many models have vegetation-specific parameters so that classification schemes are intertwined with model conceptualizations (Table 3).

Our vegetation classification (VVEG) (Table 6) was developed by considering (1) the ability of the biogeography models to produce such a common classification, (2) the ability of the biogeochemistry models to adapt their parameterizations to the classification, and (3) the vegetation classification used in extant georeferenced databases that describe the potential vegetation of the conterminous United States. Vegetation classes were defined physiognomically in terms of dominant life-form and leaf characteristics (including leaf seasonal duration, shape, and size; *Running et al.* [1994]) and, in the case of grasslands, physiologically with respect to dominance of species with the C<sub>3</sub> versus C<sub>4</sub>-photosynthetic pathway. Distribution of these types (Plate 1) was based on a gridded map of *Küchler's* [1964, 1975] potential natural vegetation (D. W. Kicklighter and A. D. McGuire, personal communication, 1995). For the purpose of this exercise, we assumed that this distribution of potential vegetation is in equilibrium with current climate.

Required soil properties, including soil texture and depth (Table 4), were based on *Kern's* [1994, 1995] 10-km gridded Soil Conservation Service national level (NATSGO) database. We used cluster analysis to group the 10-km subgrid elements into 1-4 dominant ("modal") soil types for each 0.5° cell. In this approach we represented cell soil properties by one or more dominant soil profiles, rather than by an "average soil profile" that may not correspond to an actual soil in the region. Properties of the first modal soil were used in the simulations. The models were applied to nonwetland areas (3168 total grid cells). Wetland or floodplain ecosystems were excluded because some of the models do not simulate water, carbon, or nitrogen dynamics for inundated soils.

**Climate scenarios.** Climate change scenarios used in the simulations were based on three atmospheric general circulation model (GCM) experiments for a doubled CO<sub>2</sub> atmosphere and an equilibrium climate. These were from the Geophysical Fluid Dynamics Laboratory (GFDL) [R30 2.22° x 3.75° grid run; *Manabe and Wetherald*, 1990; and *Wetherald and Manabe*, 1990], Oregon State University (OSU) [*Schlesinger and Zhao*, 1989], and United Kingdom Meteorological Office (UKMO) [*Wilson and Mitchell*, 1987] (Plate 2). In these climate sensitivity experiments, the GCMs were implemented with a simple "mixed-layer" ocean representation that includes heat storage and vertical exchange of heat and moisture with the atmosphere but omits horizontal ocean heat transport.

The three climate change scenarios were selected to represent the range of climate sensitivity over the United States among

**Table 6.** Translation of Potential Vegetation of the Conterminous United States Defined by *Küchler* [1964], to the Vegetation Classification (VVEG) Used in the VEMAP Activity

VVEG	Vegetation Type	Map Symbol
1	tundra	52
2	boreal coniferous forest	15, 21, 93, 96
3	temperate maritime coniferous forest	1, 2, 3, 4, 5, 6
4	temperate continental coniferous forest	8, 10, 11, 12, 13, 14, 16, 17, 18, 19, 20, 95
5	cool temperate mixed forest	28, 106, 107, 108, 109, 110
6	warm temperate / subtropical mixed forest	29, 89, 90, 111, 112
7	temperate deciduous forest	26, 98, 99, 100, 101, 102, 103, 104
8	tropical deciduous forest	not present
9	tropical evergreen forest	not present
10	temperate mixed xeromorphic woodland	30, 31, 32, 36, 37
11	temperate conifer xeromorphic woodland	23
12	tropical thorn woodland	not present
13	temperate deciduous savanna	61, 71, 81, 82, 84, 87, 88
14	warm temperate /subtropical mixed savanna	60, 62, 83, 85, 86
15	temperate conifer savanna	24
16	tropical deciduous savanna	not present
17	C <sub>3</sub> grasslands	47, 48, 50, 51, 63, 64, 66, 67, 68
18	C <sub>4</sub> grasslands	53, 54, 65, 69, 70, 74, 75, 76, 77
19	Mediterranean shrubland	33, 34, 35
20	temperate arid shrubland	38, 39, 40, 46, 55, 56, 57
21	subtropical arid shrubland	41, 42, 43, 44, 45, 58, 59
90	ice	not present
91	inland water bodies	no symbol
92	wetlands	49, 78, 79, 80, 92, 94, 113, 114

Vegetation types represented by map symbols 7, 9, 22, 25, 27, 72, 73, 91, 97, 105, 115, 116 are never dominant at the 0.5° longitude x 0.5° latitude grid cell resolution.

GCMs run with a mixed-layer ocean. The OSU scenario had the lowest United States average annual temperature sensitivity (+ 3.0° C) and low annual precipitation sensitivity (4% increase), and UKMO had the highest temperature (+ 6.7° C) and high precipitation sensitivity (12% increase). The GFDL R30 run had intermediate temperature (+ 4.3° C) and highest precipitation sensitivity in the mean across the United States. (21% increase). Precipitation responses in all models were regionally variable. For example, GFDL R30 showed greater than 50% increases in the southwest and 10% decreases in the southeast (Plate 2). Temperature changes were more uniform.

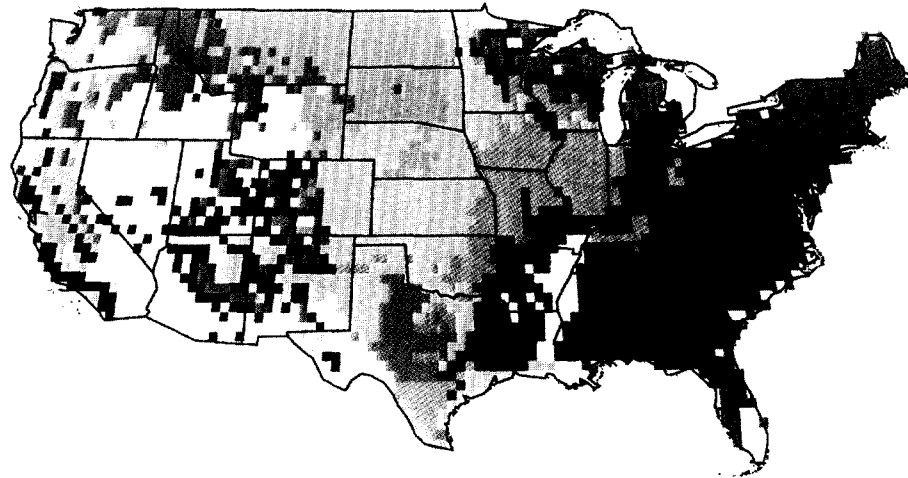
Changes in monthly mean temperature were represented as differences and those for monthly precipitation, solar radiation, and vapor pressure as change ratios. The GCM grid point change values were derived from archives at the National Center for Atmospheric Research (NCAR) [Jenne, 1992] and interpolated to the 0.5° grid (Plate 2). This provided smoothed monthly change fields that were applied to the VEMAP base climate to generate altered-climate inputs. We determined differences for relative

humidity based on the VEMAP base climate and climate changes for temperature, vapor pressure, and surface pressure. Changes in wind speed from the GCM runs were locally extreme (e.g., increases by a factor of 3 or more) and were not used in the simulations.

### Simulation Protocol

To evaluate the individual and joint effects of altered climate and doubled CO<sub>2</sub> on simulated biogeography and biogeochemistry, we implemented a factorial model experimental design (Table 7). The first set of simulation experiments was with the biogeography models. For these experiments the control runs were driven by an atmospheric CO<sub>2</sub> concentration of 355 parts per million by volume (ppmv) and monthly or daily versions of the contemporary climate data set. The subsequent sets of simulating experiments were for (1) climate change (without accompanying CO<sub>2</sub> increase) under each of the 3 GCM

## VEMAP VEGETATION DATA SET



### LEGEND

	Temp. Mixed Xeromorphic Wood.		Subtropical Arid Shrublands
	Tropical Evergreen Forest		Temperate Arid Shrublands
	Tropical Deciduous Forest		Mediterranean Shrublands
	Temperate Deciduous Forest		C4 Grasslands
	Warm Temp. Mixed/Everg. Forest		C3 Grasslands
	Cool Temp. Mixed Forest		Tropical Deciduous Savanna
	Continental Temp. Conifer Forest		Temperate Conifer Savanna
	Maritime Temp. Conifer Forest		Warm Temperate/S.T. Mixed Savanna
	Boreal Forest		Temperate Deciduous Savanna
	Tundra		Tropical Thorn Woodland
			Temp. Conifer Xeromorphic Wood.

**Plate 1.** Potential vegetation distribution of the conterminous United States based on the VEMAP vegetation classification (VVEG).

scenarios (OSU, GFDL R30, and UKMO), (2) doubled  $\text{CO}_2$  (710 ppmv), and (3) both climate and  $\text{CO}_2$  changes. The biogeography models were analyzed for their representation of potential vegetation under current and altered conditions.

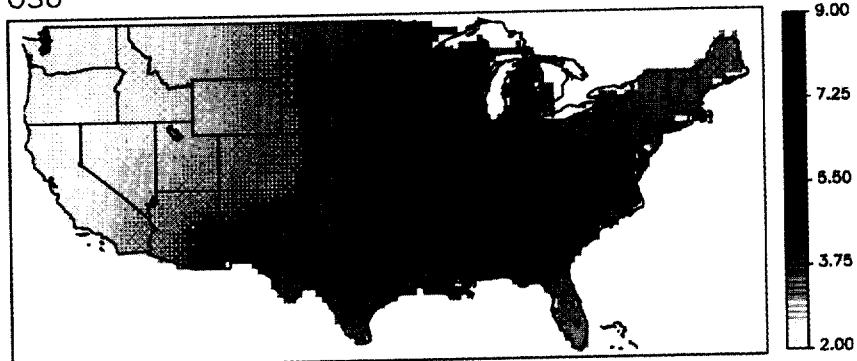
The second set of experiments was with the biogeochemistry models. Control runs with these models used the same  $\text{CO}_2$  concentration and contemporary climate data as the biogeography models and used the Küchler-derived distribution of potential vegetation (Plate 1). The biogeochemistry model sensitivity experiments were also for (1) climate change, (2) doubled  $\text{CO}_2$ , and (3) both climate and  $\text{CO}_2$  changes (Table 7).

The model results were evaluated in terms of net primary productivity (NPP), carbon in living vegetation (VEGC, including both above and belowground carbon), carbon in soil organic matter (SOILC), actual evapotranspiration (ET), and net N mineralization (NMIN).

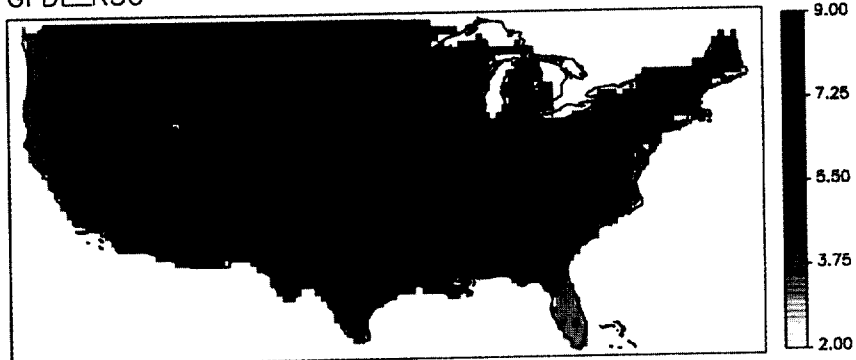
In a third set of simulations, we examined the effects of biogeographical changes on biogeochemical responses. Each biogeochemical model was run using results of the three biogeography models (Table 7). These "coupled" runs were made for contemporary (control) conditions and combined climate and doubled  $\text{CO}_2$  effects. The controls for the coupled

### Annual Temperature Change Difference

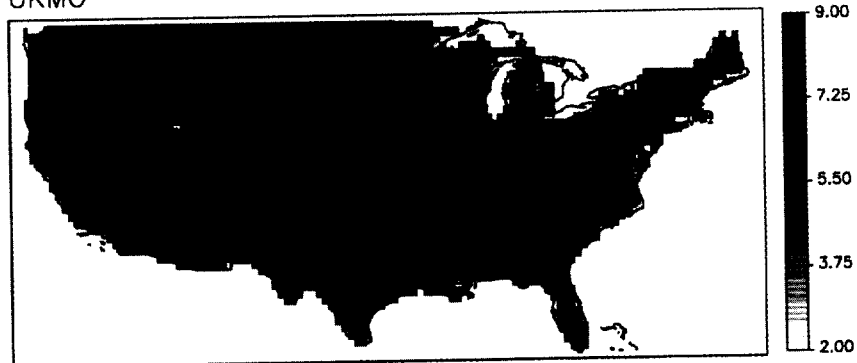
OSU



GFDL\_R30

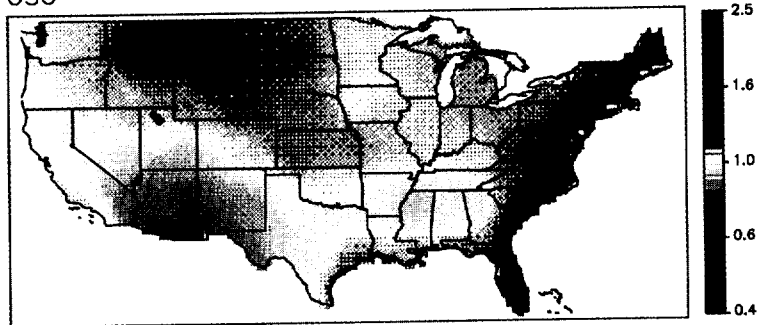


UKMO

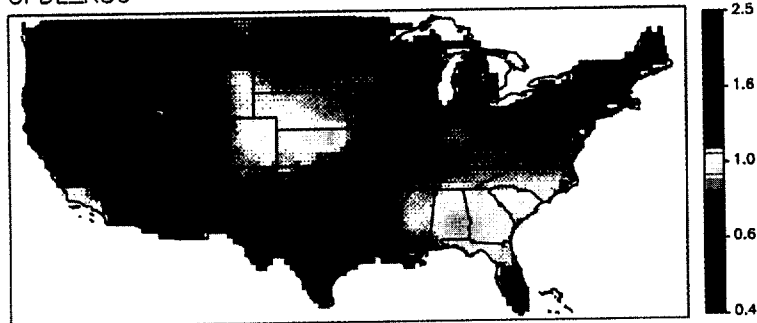


### Annual Precipitation Change Ratio

OSU



GFDL\_R30



UKMO

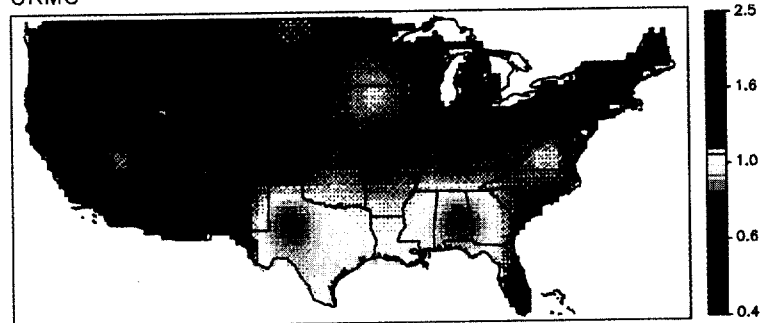


**Plate 2.** Changes in annual temperature and precipitation for doubled CO<sub>2</sub> estimated by three atmospheric general circulation models, including: Oregon State University (OSU), the Geophysical Fluid Dynamics Laboratory (GFDL R30), and the United Kingdom Meteorological Office (UKMO): (a) Absolute change in mean annual surface air temperature, and (b) Ratio of predicted to present precipitation.

**Table 7.** Factorial Design to Examine the Influence of Climate Change and Elevated Atmospheric CO<sub>2</sub> Concentration on Vegetation Distribution and the Effects of Climate, CO<sub>2</sub>, and Biome Redistribution on Biogeochemical Processes

	Biogeography Models	Biogeochemistry Models	
		With K�uchler Vegetation	With Vegetation Redistribution
Control	X	X	X
Altered climate	X	X	
Doubled CO <sub>2</sub> concentration	X	X	
Climate and CO <sub>2</sub> change	X	X	X

Control and doubled-CO<sub>2</sub> concentrations were 355 and 710 ppmv, respectively. Climate change scenarios were based on OSU, GFDL R30, and UKMO GCM experiments (see text).

runs differed from those for the independent experiments in that the vegetation fields were based on output from biogeography model control runs rather than the K uchler-derived distribution.

## Results and Discussion

### Biogeography Models

**Comparisons to the VEMAP vegetation distribution.** The three biogeography models successfully simulated the overall geographic distribution of major vegetation types under current conditions (Plate 3). We used an index known as the “kappa statistic” as a measure of map agreement: the larger the kappa statistic ( $k$ ), the greater the agreement between modeled and actual vegetation distribution [Monserud and Leemans, 1992; Prentice et al., 1992]. The three models showed nearly equal abilities to match VVEG on a cell by cell basis ( $k = 0.69$  for BIOME2, 0.70 for MAPSS, 0.72 for DOLY; Figure 1a). The models had different misclassifications with respect to individual vegetation types. One consistent model bias was to over-represent montane vegetation with respect to shrublands in the intermountain west. This bias was caused by the difficulty of representing spatial heterogeneity on a coarse grid. Climate specified for 0.5° cells in the basin-and-range topography is in effect an average of the ranges and basins, whereas the mapped vegetation is the areally predominant type, that is, commonly the arid shrublands of the basins.

**Contemporary climate and CO<sub>2</sub> concentration.** The models have similar estimates of area for forests (42 to 46% of the conterminous United States), grasslands (17 to 27%), savannas (15 to 25%), and shrublands (14 to 18%). The models differ in their placement of the boundary between C<sub>3</sub> and C<sub>4</sub> grasslands (Plate 3), reflecting the fact that these grasslands are not exclusively C<sub>3</sub> or C<sub>4</sub> systems, but rather mixtures. The models also varied in their simulations of the location and width of the ecotone between the central grasslands and eastern forests, represented by savanna types. This ecotone is hard to capture based on long-term climatic means because of its sensitivity to interannual precipitation variability and fire frequency [Borchert, 1950; Daubenmire, 1968]. Each model uses a different approach to approximate the C<sub>3</sub>/C<sub>4</sub> and forest/grassland transitions.

**Climate change.** The models' sensitivities to climate change differ in the absence of a direct CO<sub>2</sub> effect (Plate 3). All biogeography models agree in showing that the OSU scenario produces the smallest effect on biome redistribution and the UKMO produces the greatest effect. Overall, BIOME2 and MAPSS show a greater sensitivity than DOLY to the UKMO scenario (Figure 1a); and MAPSS shows a greater sensitivity than BIOME2 or DOLY to the GFDL scenario. As a result, greater divergence among the model predictions (Figure 1b) occurs when using climate scenarios with larger changes in temperature or precipitation.

The responses of forested area under climate change, but without a direct CO<sub>2</sub> effect, differ sharply among the models. The BIOME2 and DOLY models predict changes that are both negative and positive (from -18% for DOLY under OSU climate to +7% for BIOME2 under GFDL climate). The MAPSS model consistently predicts substantial decreases in forested area (from -44 to -84%). All three models predict losses in conifer forests, most extreme in MAPSS and least in BIOME2 (Figure 2a). While MAPSS predicts losses in broadleaf forests under all scenarios, BIOME2 and DOLY predict gains or losses, depending on the scenario. The three models also predict some degree of conversion of western conifer forests to broadleaf, the effect being most pronounced in BIOME2 and least in DOLY (Plate 3). In general, the conifer to broadleaf conversion is least under the OSU scenario and greatest under the UKMO scenario for all three vegetation models. The conversion to broadleaf appears to result from longer and more moist growing seasons.

Most of the simulations (Plate 3) show major northward shifts of the eastern forest belts. Warm temperate/subtropical mixed forests partly or wholly replace today's temperate deciduous forests while temperate deciduous forests partly or wholly replace cool temperate mixed forests. Tropical forests extend their range northward in the BIOME2 runs.

The models vary in their predictions of the extent to which grasslands invade forests or vice versa with climate change. The BIOME2 and MAPSS models predict that the areal extent of grasslands increases for all climate change scenarios (Figure 2a); from +4% (BIOME2 with GFDL climate) to +70% (MAPSS with UKMO). The DOLY model also predicts increases in grasslands with the OSU climate (+61%), but predicts decreases in grasslands with either the GFDL (-9%) and UKMO (-25%) climate scenarios. All three models predict eastward extensions of grasslands or savannas into the eastern broadleaf forests under

all three GCM scenarios, especially in the upper Great Lakes region of the Midwest. The greatest change occurs with the MAPSS model under the UKMO climate where almost all of the eastern forests are replaced by grasslands or savannas (Plate 3). In contrast, the DOLY model predicts only the eastward extension of savannas into the Great Lakes region with climate change. In the southern plains, the models are in general agreement; they show expansions of forests and savannas to the west under the high rainfall GFDL scenario and contractions of these types to the east under both the OSU and UKMO scenarios. Within the central grasslands, the three models also predict some degree of conversion of C<sub>3</sub> grasslands to C<sub>4</sub> grasslands because of higher temperature and/or lower moisture availability; the effect being most pronounced in BIOME2 under the UKMO climate and least pronounced in DOLY under the OSU climate.

All three biogeography models predict both positive and negative changes in the areal extent of shrublands with climate change, but differ in the magnitude and direction of these changes under a particular GCM climate (Figure 2a). Both the BIOME2 and MAPSS models predict an increase of shrublands (+9.8 and +41.5%, respectively) under the OSU climate scenario, but predict a decrease of shrublands in the warmer and wetter GFDL (-38.6% for BIOME2; -6.2% for MAPSS) and UKMO (-8.5% for BIOME2; -0.6% for MAPSS) climate scenarios. Because grasses are better able to outcompete shrubs under more moist conditions, shrublands are replaced by grasslands in these latter GCM scenarios. In contrast, the DOLY model predicts a decrease in the areal extent of shrublands for the OSU (-10.2%) and GFDL (-24.1%) scenarios, but predicts an increase of shrublands for the UKMO climate scenario (+29.5%). Within shrublands, all three models predict some degree of conversion of temperate arid shrublands to subtropical arid shrublands as a consequence of the higher temperatures under the GCM scenarios; the effect is most pronounced in DOLY under the UKMO climate and least pronounced in MAPSS or BIOME2 under the OSU climate.

**Doubled CO<sub>2</sub>.** All models show some direct effects of CO<sub>2</sub> on biome distribution in the absence of climate change. The change is least for BIOME2 (Figure 1c, doubled CO<sub>2</sub> comparisons), where the only major change is that C<sub>3</sub> grasslands increase relative to C<sub>4</sub> grasslands throughout the United States. The DOLY and MAPSS models show increases in the extent of forests through the western interior and in the prairie-forest border region.

**Climate change and doubled CO<sub>2</sub>.** A general result of considering both climate change and doubled CO<sub>2</sub> responses (Figures 1c-1d and Plate 4) is to substantially reduce the divergence among models by mitigating the climate-induced drought effects. The effect of this CO<sub>2</sub> mitigation varies among the models. The BIOME2 model predicts changes of forest area under climate change with doubled CO<sub>2</sub> that are similar to the changes of forest area under climate change alone; forests increase under the GFDL climate (+10%), but decrease under the OSU (-14%) and UKMO (-14%) climates. In contrast, the MAPSS model predicts increases in forest area under the OSU (+23%) and GFDL (+20%) climates with doubled CO<sub>2</sub> as compared to the reductions of forest area predicted under climate change alone. For the UKMO climate with doubled CO<sub>2</sub>, the MAPSS model predicts decreases in forest areas (-13%) that are much smaller than the decreases (-84%) predicted under climate

change alone. The CO<sub>2</sub> mitigation of climate-induced drought effects is also apparent in the DOLY model predictions of changes in forested area, but the effect is not as pronounced as the MAPSS model predictions; forested areas decrease under the OSU climate (-7%), but increase under the GFDL (+11%) and UKMO (+2%) climates. Within forests, the BIOME2 and DOLY models still predict overall losses of western conifer forests under all three GCM scenarios while the MAPSS model predicts losses of conifer forests only under the UKMO climate (Figure 2b). The MAPSS model predicts increases in conifer forests under both the OSU and GFDL climates.

As forested areas are generally predicted to increase under climate change with doubled CO<sub>2</sub>, the biogeography models predict either smaller increases or decreases in the areal extent of grasslands in comparison to climate change alone (Figure 2b). Both the BIOME2 and DOLY models predict that grasslands increase under the OSU climate (+10% for BIOME2; +48% for DOLY) and decrease under the GFDL climate (-5% for BIOME2; -8% for DOLY), but the models differ in their response for the UKMO climate (+39% for BIOME2; -31% for DOLY). Unlike the scenarios of climate change alone, the MAPSS model predicts that grasslands will decrease for all climate scenarios with doubled CO<sub>2</sub>. The models still predict eastward extensions of grasslands or savannas into the eastern broadleaf forests under all three GCM scenarios, but these extensions are more limited than predicted by the climate change alone scenarios; especially the changes predicted by the MAPSS model. The response of grassland composition differs among the models. Climate change alone generally favors C<sub>4</sub> grasses in all models. However, in BIOME2 this effect is reversed by the CO<sub>2</sub> fertilization of C<sub>3</sub> grasses, which allows C<sub>3</sub> grasslands to spread southward to Texas.

With climate change and elevated CO<sub>2</sub>, all biogeography models predict the areal extent of shrublands to decrease for all GCM climates (from -75% for MAPSS under GFDL climate to -2% for DOLY under UKMO climate), with the exception of BIOME2 under the OSU climate which predicts increases in shrublands (+14%). Within shrublands, DOLY still predicts large increases in subtropical arid shrublands (+30 to +185%); BIOME2 predicts gains or losses (-30 to +74%); and MAPSS predicts losses or small gains (-56 to +2%). With increased water use efficiency from elevated CO<sub>2</sub>, grasses are more able to gain a competitive advantage over shrubs to reduce the areal extent of shrublands. Clearly for all biomes, the three biogeography models exhibit complex water balance responses, combining sensitivities to increases in temperature and rainfall with increased water use efficiency from elevated CO<sub>2</sub>.

### Biogeochemistry Models

**Contemporary climate and CO<sub>2</sub> concentration.** The continental-scale estimates of annual NPP for contemporary climate at an atmospheric concentration of 355 ppmv CO<sub>2</sub> vary between 3125 x 10<sup>12</sup> gC (TgC) yr<sup>-1</sup> and 3772 TgC yr<sup>-1</sup> (Table 8). This range is equivalent to the measurement error in NPP. The estimates for total carbon storage vary between 108 x 10<sup>15</sup> gC (PgC) and 118 PgC (Table 8), which represents a 9% difference among the models. Although the continental-scale estimates of total carbon storage are similar among the models, BIOME-BGC

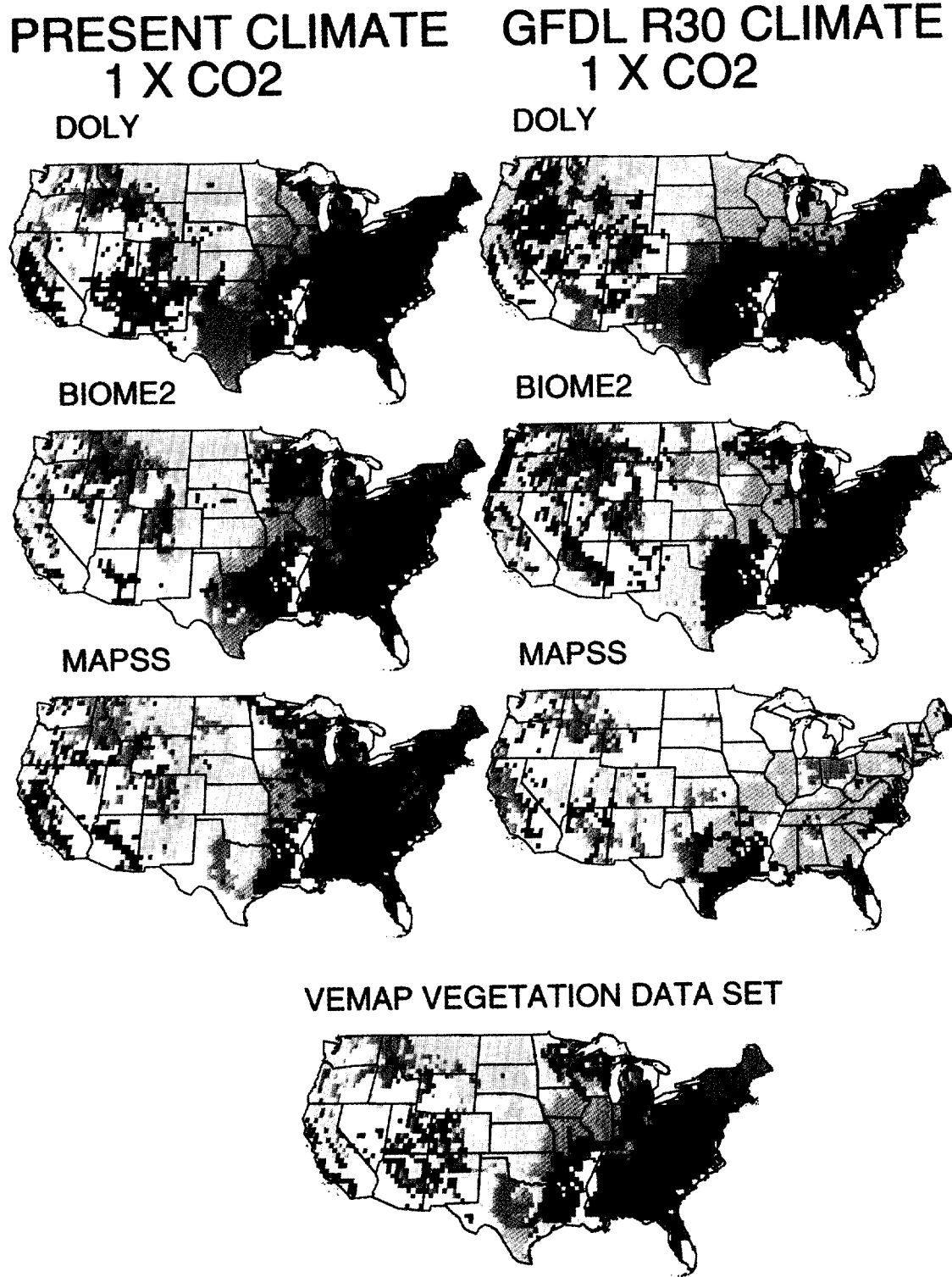


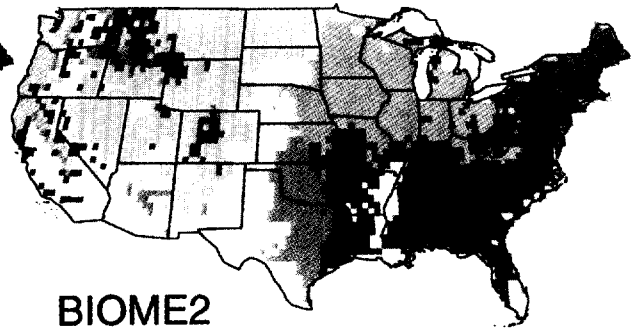
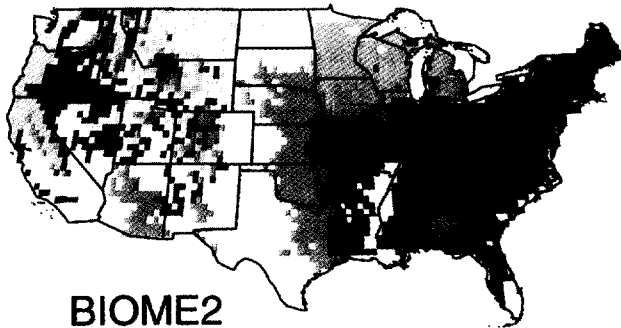
**Plate 3.** The effect of climate change on vegetation distribution. The simulated vegetation distributions of the three biogeography models (DOLY, BIOME2, and MAPSS) are compared to the VEMAP vegetation distribution and four climate scenarios: contemporary, OSU, GFDL R30, and UKMO. All simulations are based on an atmospheric CO<sub>2</sub> concentration of 355 ppmv.

# UKMO CLIMATE 1 X CO2

# OSU CLIMATE 1 X CO2

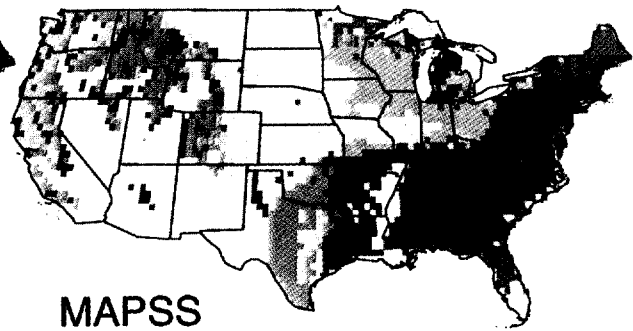
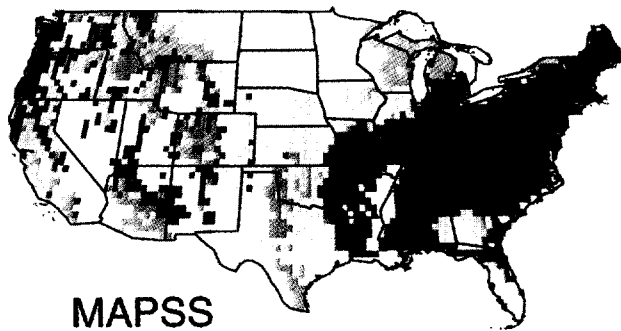
DOLY

DOLY



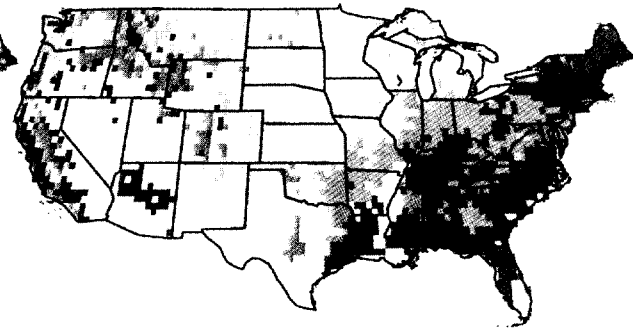
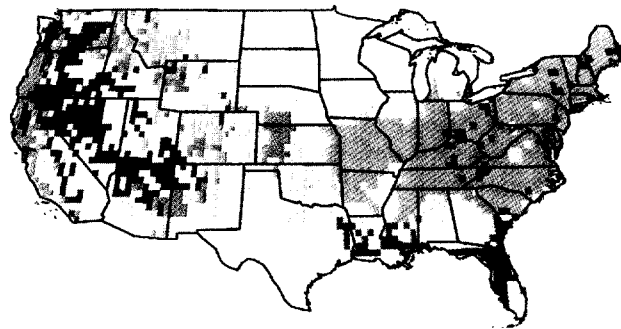
BIOME2

BIOME2



MAPSS

MAPSS



## LEGEND

- Temp. Mixed Xeromorphic Wood.
- Tropical Evergreen Forest
- Tropical Deciduous Forest
- Temperate Deciduous Forest
- Warm Temp. Mixed/Everg. Forest
- Cool Temp. Mixed Forest
- Continental Temp. Conifer Forest
- Maritime Temp. Conifer Forest
- Boreal Forest
- Tundra

- Subtropical Arid Shrublands
- Temperate Arid Shrublands
- Mediterrean Shrublands
- C4 Grasslands
- C3 Grasslands
- Tropical Deciduous Savanna
- Temperate Conifer Savanna
- Warm Temperate/S.T. Mixed Savanna
- Temperate Deciduous Savanna
- Tropical Thorn Woodland
- Temp. Conifer Xeromorphic Wood.

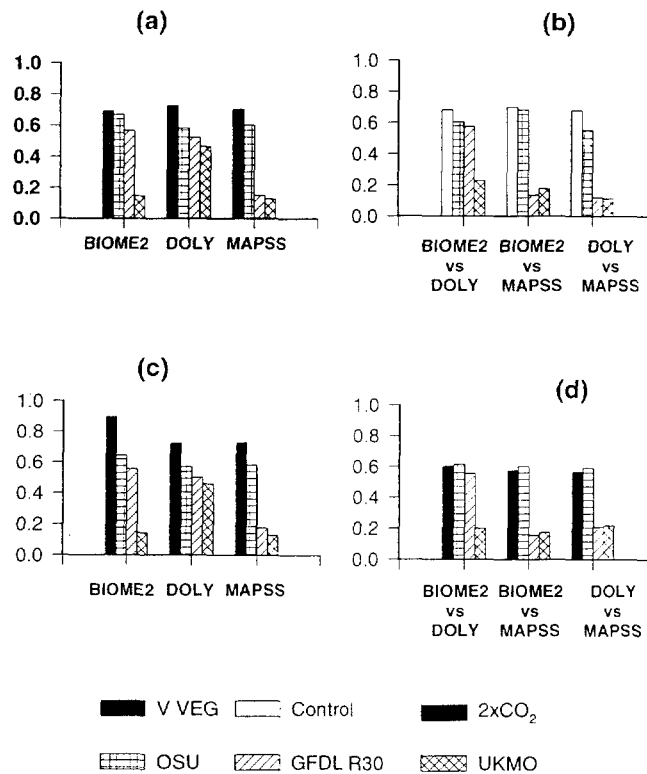


**Figure 1.** Comparison of the kappa statistics among the VEMAP vegetation distribution (VVEG) and the simulated vegetation distributions of the three biogeography models (BIOME2, MAPSS, and DOLY) for various climate scenarios and atmospheric CO<sub>2</sub> scenarios: (a) the simulated vegetation distribution using current climate (Control) at an atmospheric CO<sub>2</sub> concentration of 355 ppmv is compared to the VEMAP vegetation distribution and the simulated vegetation distributions of the three biogeography models using the OSU, GFDL R30, and UKMO climates at an atmospheric CO<sub>2</sub> concentration of 355 ppmv; (b) the relative agreement between pairs of biogeography models for various climate scenarios at an atmospheric CO<sub>2</sub> concentration of 355 ppmv; (c) the simulated vegetation distribution using current climate (Control) at an atmospheric CO<sub>2</sub> concentration of 355 ppmv is compared to the simulated vegetation distributions of the three biogeography models using current, OSU, GFDL R30, and UKMO climates at an atmospheric CO<sub>2</sub> concentration of 710 ppmv; and (d) the relative agreement between pairs of biogeography models for various climate scenarios at an atmospheric CO<sub>2</sub> concentration of 710 ppmv. Large values of the kappa statistic indicate good agreement between vegetation distributions.

estimates higher soil carbon (70 PgC) than the other two models (52 PgC by CENTURY and 49 PgC by TEM) and lower vegetation carbon (48 PgC) than either CENTURY (64 PgC) or TEM (59 PgC). The ecosystem level estimates of NPP and total carbon storage are highly correlated ( $P < 0.0001$ ;  $N = 17$  ecosystems) among the models; in pairwise comparisons among the models the correlations range from 0.907 to 0.958 for NPP and from 0.954 to 0.970 for total carbon storage. The estimates for individual grid cells are also highly correlated ( $P < 0.0001$ ;  $N = 3168$  grid cells) among the models; correlations range from 0.777 to 0.848 for NPP and 0.818 to 0.911 for carbon storage.

**Climate change.** The continental level NPP responses of CENTURY and TEM to climate change are positive (Table 8) because both models estimate that nitrogen mineralization increases for the three climates (CENTURY, 10 to 19%, TEM, 8 to 11%). Enhanced nitrogen mineralization increases the amount of nitrogen available to plants so that NPP may increase. For CENTURY, the response of NPP and nitrogen mineralization is lowest for the low-temperature OSU scenario and highest for the high-temperature UKMO scenario. The CENTURY-estimated NPP of warm temperate/subtropical mixed forest under the UKMO scenario increases 11%, and is associated with a 10% increase in nitrogen mineralization rates. Total carbon storage in CENTURY is enhanced by 4% for all climate scenarios (Table 8). Although CENTURY estimates losses of soil C for all these climate scenarios, gains in vegetation C were 2 to 3 times as large as these losses.

In contrast to CENTURY, the NPP increases of TEM (Table 8) are highest for the low-temperature OSU scenario (10%) and lowest for the high-temperature UKMO scenario (7%). The TEM estimates enhanced evaporative demand in warm temperate/subtropical mixed forest under the UKMO scenario, and predicts lower nitrogen cycling for UKMO than for OSU. Under the UKMO scenario, NPP for warm temperate/subtropical mixed forest decreases by 10%, which is associated with a 12% decrease in nitrogen mineralization. The response of total carbon storage is correlated with the pattern of NPP response and ranges from 1% increase for OSU to 11% decrease for UKMO (Table 8). Thus although the NPP responses of TEM and CENTURY both depend on the response of nitrogen cycling to climate change, the models differ in how temperature and moisture availability influence nitrogen mineralization rates.

Among the three biogeochemistry models, BIOME-BGC generally estimates the most negative or smallest positive NPP responses to climate change (Table 8). The decrease in NPP for the UKMO scenario is primarily caused by lower production in warm temperate/subtropical mixed forest where mean annual air temperature increases 6.4°C and radiation increases 5.8%, but precipitation increases only 1.7%; the decrease in NPP is caused by increased evaporative demand. The model simulated increases in NPP for the GFDL scenario as a result of reduced simulated evaporative demand for the GFDL scenario. The NPP response for the OSU scenario is intermediate because the low continental precipitation increase (4.3%) that is associated with low increases in temperature (+3.0°C) and solar radiation (1.6%) causes evaporative demand to increase slightly in the BIOME-BGC. The decreases in total carbon storage by BIOME-BGC range from 38% reduction for UKMO to 17% reduction for OSU (Table 8). For BIOME-BGC estimates of total carbon storage to changes in climate are caused by decreases in NPP because of decreased water availabilities, and increases in plant and soil respiration because of higher temperatures. Soil C loss accounts for 72 to 85% of the total C loss across the three climate scenarios.

**Doubled CO<sub>2</sub>.** Doubled atmospheric CO<sub>2</sub> causes continental-scale increases in NPP that range from 5% in CENTURY to 11% in BIOME-BGC; TEM estimates an intermediate increase of 9% (Table 8). These increases are substantially lower than the 25 to 50% growth response to doubled CO<sub>2</sub> that has been observed in greenhouse studies that provide plants with sufficient nutrients and water [Kimball, 1975; Gates, 1985]. Total carbon storage

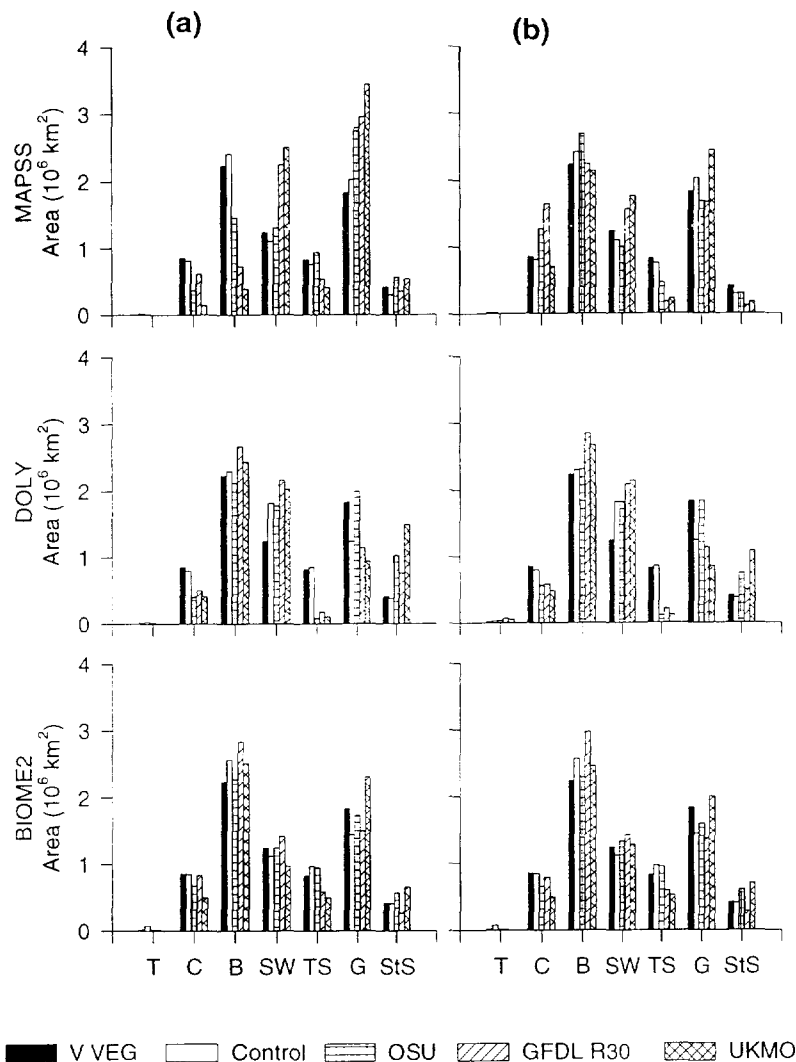


**Figure 2.** Comparison of area estimates of different biomes under various climate scenarios as simulated by three different vegetation distribution models: (a) without physiological  $\text{CO}_2$  effects; and (b) with physiological  $\text{CO}_2$  effects. The control simulations in Figure 2b do not include a  $\text{CO}_2$  effect. The vegetation classes are aggregated from the original 21 VVEG types as follows: Tundra (T), 1; Conifer Forests (C), 2-4; Broadleaf Forests (B), 5-9; Savanna/Woodland (SW), 10, 11, 13-16; Subtropical Shrub/Steppe (StS), 12,21; Temperate Shrub/Steppe (TS), 19,21; and Grasslands (G), 17,18.

increased between 2% in CENTURY and 9% in TEM, with an intermediate 7% in BIOME-BGC. For all three models, carbon storage increases more in vegetation than soils (57 to 67% in vegetation).

Significant dissimilarities in ecosystem level responses are caused, primarily, by different mechanisms controlling the  $\text{CO}_2$  response of carbon assimilation by the vegetation. In BIOME-BGC, photosynthetic capacity is reduced because of a prescribed lower leaf nitrogen concentration, but increased intercellular  $\text{CO}_2$  potentially enhances carbon uptake. In contrast, the response of carbon capture in the other two models is primarily controlled by nitrogen feedbacks. In TEM the ability of vegetation to incorporate elevated  $\text{CO}_2$  into production is controlled by stoichiometric constraints on the C:N ratios of production and vegetation stocks. Also in TEM, elevated  $\text{CO}_2$  enhances

continental-scale nitrogen uptake by the vegetation by 10% in response to doubled  $\text{CO}_2$ . In CENTURY, doubled  $\text{CO}_2$  results in a prescribed 20% reduction in transpiration which potentially modifies soil moisture levels. An additional effect in CENTURY is a 20% increase in the C:N ratio of vegetation. In contrast to TEM, continental-scale nitrogen mineralization in CENTURY decreases by 2% in response to doubled  $\text{CO}_2$  because of slower decomposition resulting from changes in foliar N.

**Climate change and doubled  $\text{CO}_2$ .** The NPP and total carbon responses of BIOME-BGC and CENTURY to changes in both climate and  $\text{CO}_2$  are essentially additive (Table 8). In TEM an interaction between elevated  $\text{CO}_2$  and climate that influences NPP and carbon storage is caused by enhanced plant N uptake. This  $\text{CO}_2$  and climate change interaction ranges from 8% in the OSU scenario to 19% in the UKMO scenario and results in

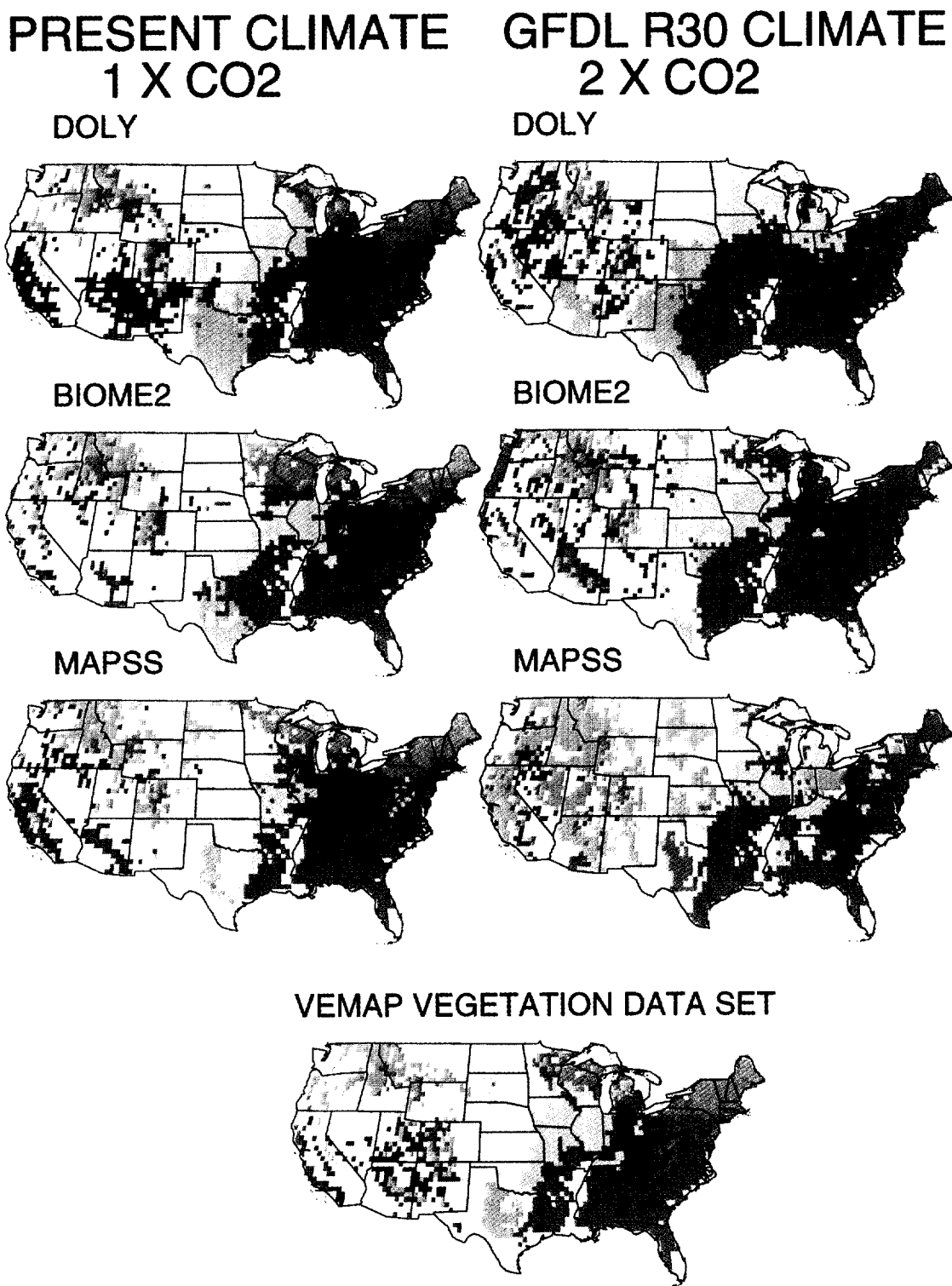


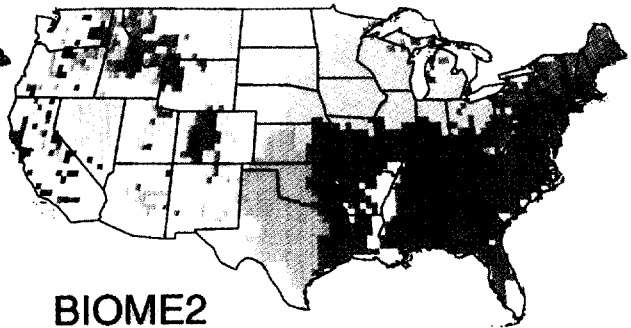
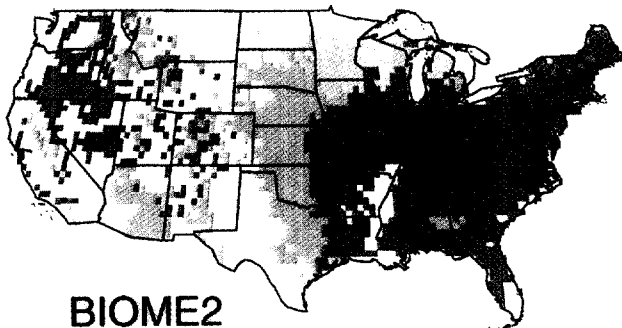
**Plate 4.** The effect of climate change and doubled CO<sub>2</sub> on vegetation distribution. The simulated vegetation distributions of the three biogeography models (DOLY, BIOME2, and MAPSS) are compared to the VEMAP vegetation distribution and four climate scenarios: contemporary, OSU, GFDL R30, and UKMO. The vegetation distribution for the contemporary climate is based on an atmospheric CO<sub>2</sub> concentration of 355 ppmv. The vegetation distributions for the other climate scenarios are based on an atmospheric CO<sub>2</sub> concentration of 710 ppmv.

# UKMO CLIMATE 2 X CO2

# OSU CLIMATE 2 X CO2

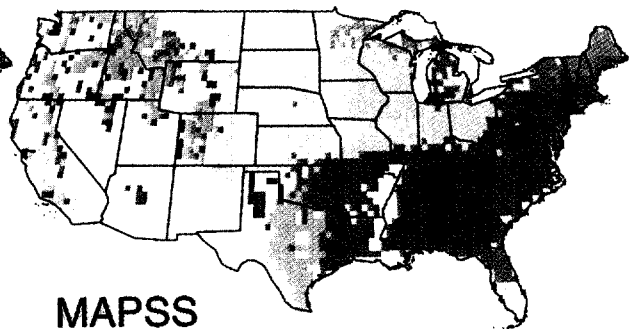
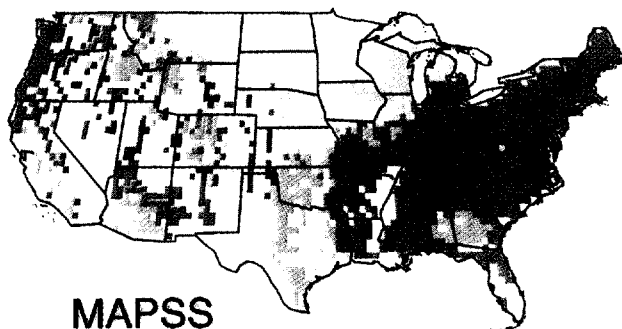
DOLY

DOLY



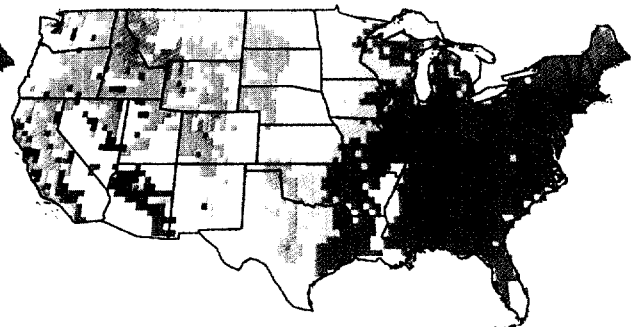
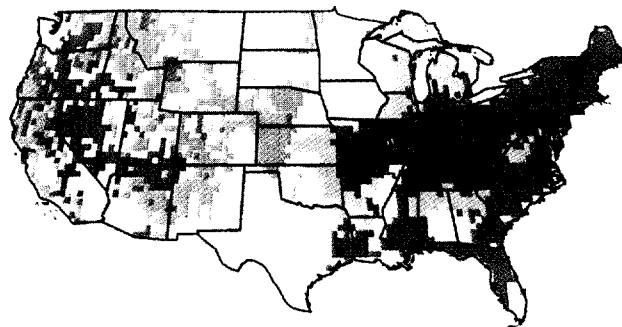
BIOME2

BIOME2



MAPSS

MAPSS



## LEGEND

-  Temp. Mixed Xeromorphic Wood.
-  Tropical Evergreen Forest
-  Tropical Deciduous Forest
-  Temperate Deciduous Forest
-  Warm Temp. Mixed/Everg. Forest
-  Cool Temp. Mixed Forest
-  Continental Temp. Conifer Forest
-  Maritime Temp. Conifer Forest
-  Boreal Forest
-  Tundra

-  Subtropical Arid Shrublands
-  Temperate Arid Shrublands
-  Mediterranean Shrublands
-  C4 Grasslands
-  C3 Grasslands
-  Tropical Deciduous Savanna
-  Temperate Conifer Savanna
-  Warm Temperate/S.T. Mixed Savanna
-  Temperate Deciduous Savanna
-  Tropical Thorn Woodland
-  Temp. Conifer Xeromorphic Wood.

**Table 8.** Continental-Scale Responses of Net Primary Production and Total Carbon Storage (Vegetation plus Soils) to Doubled CO<sub>2</sub>, Climate Change, and Doubled CO<sub>2</sub> plus Climate Change as estimated by BIOME-BGC (BBGC), CENTURY (CEN), and the Terrestrial Ecosystem Model (TEM)

	Annual Net Primary Production (10 <sup>12</sup> gC yr <sup>-1</sup> or percent response)			Total Carbon Storage (10 <sup>15</sup> gC or percent response)		
	BBGC	CEN	TEM	BBGC	CEN	TEM
Baseline estimates	3772	3125	3225	118	116	108
Response to climate change at 1XCO <sub>2</sub>						
OSU	-2.9%	+8.8%	+10.3%	-16.9%	+3.5%	+1.4%
GFDL	+9.2%	+15.5%	+8.3%	-18.4%	+3.5%	-4.6%
UKMO	-6.5%	+17.0%	+6.6%	-37.6%	+4.3%	-10.9%
Response to 2XCO <sub>2</sub>	+10.8%	+5.0%	+8.7%	+6.5%	+2.2%	+8.5%
Response to climate change at 2XCO <sub>2</sub>						
OSU	+9.4%	+14.6%	+26.5%	-9.1%	+5.9%	+16.1%
GFDL	+20.2%	+22.1%	+30.5%	-11.0%	+6.1%	+14.6%
UKMO	+1.7%	+23.6%	+34.6%	-32.7%	+7.2%	+12.3%
Interaction term between response to 2XCO <sub>2</sub> , climate, and 2XCO <sub>2</sub> plus climate						
OSU	+1.5%	+0.9%	+7.5%	+1.4%	+0.1%	+6.2%
GFDL	+0.2%	+1.6%	+13.5%	+0.9%	+0.3%	+10.7%
UKMO	-2.6%	+1.7%	+19.4%	-1.6%	+0.8%	+14.7%

overall increases that range from 27 to 35% (Table 8), with similar effects for carbon storage (Table 8). Because of the interaction between elevated  $\text{CO}_2$  and climate responses, TEM estimates the greatest enhancement in NPP and total carbon storage among the three biogeochemistry models.

### Coupled Models

The coupled-model experiments involve spatially extrapolating the biogeochemistry models for the vegetation distributions that are defined by the biogeography models for each of three GCM-generated climate scenarios. A coupling of one biogeochemistry model with the vegetation of one biogeography model is hereafter referred to as a "model pair". The biogeochemistry models did not determine the transient changes in NPP or carbon storage as vegetation changed on a grid cell. Instead, the biogeochemistry models simulated the equilibrium fluxes and pools for the new vegetation and climate of the grid cell. For example, a grid cell that changed from a  $\text{C}_3$  grassland to a temperate deciduous forest used the parameters associated with temperate deciduous forests.

#### NPP and total carbon storage for contemporary climate.

For contemporary climate at 355 ppmv  $\text{CO}_2$ , NPP for the three modeled vegetations varies among the biogeochemistry models from 3132  $\text{TgC yr}^{-1}$  (CENTURY with MAPSS vegetation) to 3854  $\text{TgC yr}^{-1}$  (BIOME-BGC with BIOME2 vegetation) (Table 9). The range is similar to that estimated among the three biogeochemistry models for the VEMAP vegetation distribution (Table 8). Thus the NPP estimates for a given biogeochemistry model are relatively constant among the different current vegetation distributions, with most of the variability attributable to differences among the biogeochemistry models. Estimates for total carbon storage for the three current vegetation distributions range from 109 PgC (TEM with MAPSS vegetation) to 125 PgC (CENTURY with BIOME2 vegetation) (Table 9). Similar to NPP, most of the variability is attributable to differences among the biogeochemistry models.

**NPP responses to climate change and elevated carbon dioxide.** The total continental-scale response of NPP is calculated for each model pair by subtracting the NPP estimate for contemporary climate at 355 ppmv  $\text{CO}_2$ , from that for the future climate at doubled  $\text{CO}_2$ ; and is relative to the estimate for contemporary climate (Table 9). The total NPP responses are positive for most of the model pairs, but range widely. There are no relative increases in NPP when BIOME-BGC is run with either the DOLY or MAPSS vegetations for the UKMO climate (Table 9, Plate 5). The DOLY model simulates little change in the forested area of the United States (42 to 43%), whereas MAPSS simulates a decrease from 44 to 38%. The largest NPP increases occur when the TEM is run with the MAPSS vegetation for the OSU climate (40%). The MAPSS model estimates that the forested area of the conterminous United States increases from 44 to 53% under the OSU climate.

The total continental-scale NPP response for a model pair can be partitioned into two components (Table 10) (1) those resulting from changes in area of ecosystems (i.e., structural responses), and (2) those resulting from a change in mean NPP for an ecosystem type based on the predictions of the biogeochemistry models (i.e., functional responses). The structural response for a

vegetation type is determined by multiplying its mean contemporary NPP (grams carbon per square meter per year) times the change in area estimated by the biogeography model. The continental-scale structural response for the model pair is determined by summing the structural response of all vegetation types. The functional NPP response is determined by subtracting the structural response from the total response.

The structural response of NPP is generally positive because in most cases the biogeography models predict expansion of high NPP ecosystems at the expense of low NPP ecosystems. The functional NPP responses are specific to each biogeochemistry model: BIOME-BGC's range from -22% (DOLY for UKMO climate) to 7% (BIOME2 for OSU climate), CENTURY's are almost always positive with the largest being 14% (BIOME2 for UKMO climate), and TEM's are always positive with the largest being 31% (BIOME2 for OSU climate). The structural responses of BIOME-BGC with all three biogeography model vegetations for the UKMO climate are effectively canceled by the functional NPP response of BIOME-BGC to the UKMO climate. In contrast, the structural responses of NPP for the pairing of TEM with all three biogeography model vegetations for the UKMO climate are enhanced by the functional responses of TEM to this climate. There are two aspects to the mechanism underlying the functional NPP response of TEM; increased nitrogen mineralization in response to elevated temperature, and increased nitrogen uptake. For model pairs involving either BIOME-BGC or CENTURY, the structural responses are generally equal to or greater than the functional responses (Table 10). In contrast, for model pairs involving TEM, the structural responses are generally less than the functional responses.

#### Carbon storage responses to climate change and elevated carbon dioxide.

For the model pairs, both positive and negative changes of total carbon storage occur (Table 9). Similar to NPP, the responses of carbon storage range widely and depend on the combination of climate scenario and model linkages. The largest carbon storage reduction, -39%, occurs when BIOME-BGC is run with the MAPSS vegetation for the UKMO climate (Table 9, Plate 6). This is an absolute loss of 47 PgC, of which 33 Pg (70%) is from soil and 14 Pg (30%) is from vegetation. At the other extreme, the largest positive responses of carbon storage, an increase of 32%, occur when TEM is run with the MAPSS vegetations for the OSU and GFDL climates (Table 9). For the GFDL climate, this is an absolute increase of 35 PgC, of which 5% is in soils and 95% is in vegetation.

The structural and functional responses for total carbon storage are calculated analogous to those for NPP. Both positive and negative structural responses occur (Table 10) and reflect changes in forest area predicted by the biogeography models. Similar to the NPP functional responses, those of total carbon storage are specific to the different biogeochemistry models: BIOME-BGC's are always negative; CENTURY's are always small and can be either positive or negative; and TEM's are always positive with the largest being 23%. The largest total carbon storage reduction, -39%, occurs when BIOME-BGC is run with the MAPSS vegetation for the UKMO climate. The decrease in forested area from 44 to 38% under this vegetation is responsible for the structural response. The functional response indicates a large reduction in carbon density within the forests. The reduction is caused by a combination of lower NPP due to water stress and higher plant respiration and decomposition

caused by elevated temperature. In BIOME-BGC the  $Q_{10}$  for the decomposition relationship is 2.4 as compared to approximately 2.0 in CENTURY and TEM; the  $Q_{10}$ 's for plant respiration are similar among the three models (2.0).

The largest total carbon storage increase, 32%, occurs when TEM is run with the MAPSS vegetation for the OSU climate (Table 10) and is caused by an expansion of forests from 44 to 53% of the continental United States and temperature-enhanced nitrogen cycling. This forest expansion primarily replaces the shrublands.

## Implications

The response of ecosystems to changing climate is a central scientific issue for (1) understanding past states of the Earth's land surface and carbon cycle, (2) explaining the current state of ecosystems, and (3) predicting potential future responses to environmental change. While the first two issues are fundamental to ecological understanding and to establishing the credibility of predictive models, the third one is important for policy makers considering the needs for greenhouse gas emission controls, and possible adaptation strategies. An objective of VEMAP was to provide preliminary information concerning the potential responses of terrestrial ecosystems to climate change. The VEMAP exercise allowed us to identify common responses of models and important differences. Where the models differ in their predictions, they reveal areas where our lack of understanding of certain fundamental ecological processes limits our ability to narrow the range of predictions, and points to areas of research that could reduce uncertainties. The highly structured nature of the intercomparison allowed rigorous intercomparison of results, but also constrained the range of questions explored. With VEMAP as a basis for understanding, future studies can explore a wider range of questions, and implement more realistic conditions.

The VEMAP activity represents the state-of-the-art in terms of capabilities to project possible ecological effects of climate change and elevated atmospheric  $CO_2$  levels, and the projections can begin to provide policy makers with some sense of the sensitivity of natural ecosystems in the United States to these changes. The results clearly indicate that important properties of ecosystems, including the actual distribution of major vegetation types, and such critical functional responses as primary productivity and carbon storage, could be highly sensitive to the magnitude of climatic change that is predicted by some GCMs. However, there is considerable variation among models in the magnitude and even direction of change.

Perhaps the most important messages that should be taken from the VEMAP exercise pertain to the identification of priorities for future research. We have identified the following four broad areas of research as ones deserving immediate attention.

## Modularization of Models

We think that converting all of the models to a modular structure will facilitate model comparisons and pairings. For a

**Table 9.** Annual Net Primary Production (NPP) and Total Carbon Storage for the Linkage of the Three Biogeochemistry Models (BGC) (BIOME-BGC (BBGC), CENTURY (CEN), and the Terrestrial Ecosystem Model (TEM)) with the Vegetation Distributions of the Three Biogeography Models (VEG) (BIOME2, DOLY and MAPSS) for Contemporary Climate (CON) at 355 ppmv  $CO_2$  and Three GCM Climates (OSU, GFDL, and UKMO) at 710 ppmv  $CO_2$

Models	Annual NPP ( $10^{12}$ gC yr <sup>-1</sup> or percent response)					Total Carbon Storage ( $10^{15}$ gC or percent response)				
	BGC	VEG	CON	OSU	GFDL	UKMO	CON	OSU	GFDL	UKMO
BBGC	BIOME2		3854	+7.4%	+21.7%	+0.4%	122	-13.2%	-9.5%	-34.7%
	DOLY		3834	+5.6%	+20.1%	-0.1%	122	-18.1%	-13.6%	-36.4%
	MAPSS		3798	+11.9%	+20.4%	-0.7%	120	-8.3%	-13.9%	-39.4%
CEN	BIOME2		3200	+11.3%	+18.4%	+12.2%	125	-0.8%	+12.6%	-1.8%
	DOLY		3258	+26.0%	+20.4%	+14.7%	124	+9.8%	+17.7%	+7.8%
	MAPSS		3132	+15.6%	+29.2%	+20.3%	120	+17.0%	+20.4%	-1.5%
TEM	BIOME2		3289	+27.0%	+38.5%	+27.8%	114	+11.9%	+25.7%	0.0%
	DOLY		3298	+33.1%	+39.0%	+33.2%	114	+19.7%	+25.3%	+12.5%
	MAPSS		3288	+39.7%	+37.2%	+32.4%	109	+32.3%	+32.2%	+1.7%

# Net Primary Productivity, Change from Contemporary

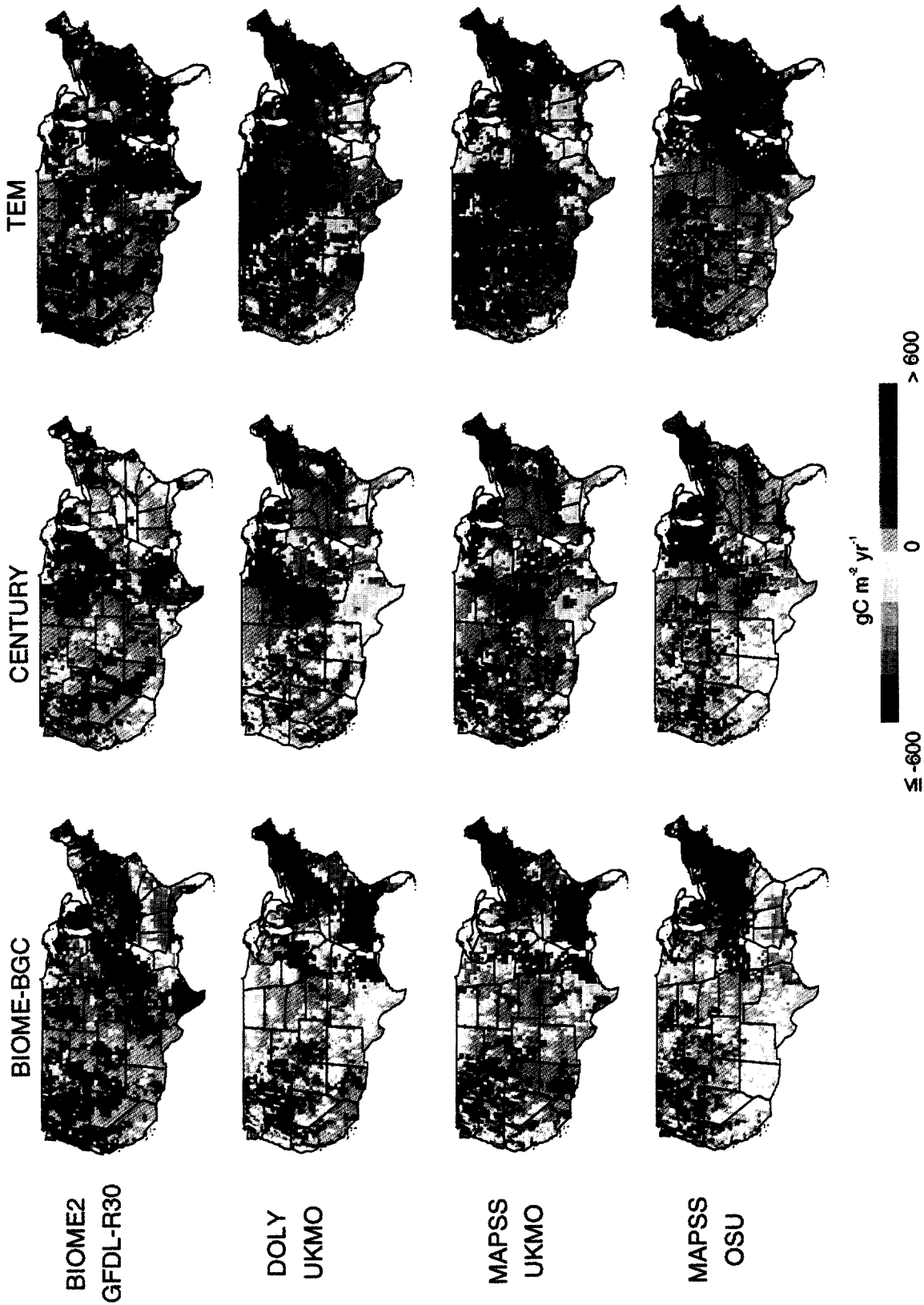


**Plate 5.** Comparison of changes in annual net primary productivity (NPP) estimated when biogeochemistry models (BIOME-BGC, CENTURY, TEM) are run with the vegetation distributions of the biogeography models (BIOME2, DOLY, MAPSS) for particular climate scenarios (GFDL R30, UKMO, OSU).

**Table 10.** The Total, Structural, and Functional Responses of Annual Net Primary Production (NPP) and Total Carbon Storage for the Linkage of the Three Biogeochemistry Models (BGC) (BIOME-BGC (BBGC), CENTURY (CEN), and the Terrestrial Ecosystem Model (TEM)) with the Vegetation Distributions of the Three Biogeography Models (VEG) (BIOME2, DOLY and MAPSS) for Contemporary Climate (CON) for the Three GCM Climates (OSU, GFDL, and UKMO) at 710 ppmv CO<sub>2</sub>

BGC	Models	VEG	Response				Annual NPP (10 <sup>12</sup> gC yr <sup>-1</sup> or percent response)				Total Carbon Storage (10 <sup>15</sup> gC or percent response)			
			CON	OSU	GFDL	UKMO	CON	OSU	GFDL	UKMO	CON	OSU	GFDL	UKMO
BBGC	BIOME2	Total Structural Functional	3854	+7.4%	+21.7%	+0.4%	122	-13.2%	-9.5%	-34.7%				
			3834	+5.6%	+20.1%	+7.1%	122	-10.5%	+7.9%	-13.9%				
BBGC	DOLY	Total Structural Functional	3834	+11.3%	+28.3%	+21.8%	120	-18.1%	-13.6%	-36.4%				
			3798	-5.7%	-8.4%	-21.9%	120	-5.9%	+5.0%	-4.0%				
BBGC	MAPSS	Total Structural Functional	3200	+11.9%	+20.4%	-0.7%	125	-8.3%	-13.9%	-39.4%				
			3258	+16.6%	+17.6%	+8.1%	125	+8.6%	+7.5%	-12.6%				
CEN	BIOME2	Total Structural Functional	3132	-4.7%	+2.8%	-8.8%	124	-16.9%	-21.4%	-26.8%				
			3289	+11.3%	+18.4%	+12.2%	114	-0.8%	+12.6%	-1.8%				
CEN	DOLY	Total Structural Functional	3288	-2.1%	+14.5%	-2.3%	114	-5.1%	+14.8%	-2.3%				
			3298	+13.4%	+3.9%	+14.5%	114	+4.3%	-2.2%	+0.5%				
CEN	MAPSS	Total Structural Functional	3288	+26.0%	+20.4%	+14.7%	120	+9.8%	+17.7%	+7.8%				
			3132	+12.5%	+22.0%	+15.1%	120	+2.8%	+17.7%	+11.3%				
TEM	BIOME2	Total Structural Functional	3289	+13.5%	-1.6%	-0.4%	114	+7.0%	0.0%	-3.5%				
			3298	+15.6%	+29.2%	+20.3%	114	+17.0%	+20.4%	-1.5%				
TEM	DOLY	Total Structural Functional	3288	+12.6%	+22.7%	+10.8%	114	+16.5%	+23.3%	-2.1%				
			3298	+3.0%	+6.5%	+9.5%	114	+0.5%	-2.9%	+0.6%				
TEM	MAPSS	Total Structural Functional	3288	+27.0%	+38.5%	+27.8%	109	+11.9%	+25.7%	0.0%				
			3298	-3.8%	+11.6%	-0.4%	109	-9.2%	+11.7%	-9.7%				
TEM	DOLY	Total Structural Functional	3288	+30.8%	+26.9%	+28.2%	109	+21.1%	+14.0%	+9.7%				
			3298	+33.1%	+39.0%	+33.2%	109	+19.7%	+25.3%	+12.5%				
TEM	MAPSS	Total Structural Functional	3288	+6.0%	+17.6%	+13.1%	109	-3.0%	+9.6%	+1.4%				
			3298	+27.1%	+21.4%	+20.1%	109	+22.7%	+15.7%	+11.1%				
TEM	DOLY	Total Structural Functional	3288	+39.7%	+37.2%	+32.4%	109	+32.3%	+32.2%	+1.7%				
			3298	+10.9%	+13.7%	+8.7%	109	+9.6%	+14.9%	-6.9%				
TEM	MAPSS	Total Structural Functional	3288	+28.8%	+23.5%	+23.7%	109	+22.7%	+17.3%	+8.6%				
			3298				109							

The reference for the responses are the estimates of the biogeochemistry models for the vegetation distributions of the biogeography models at contemporary climate (CON) and 355 ppmv CO<sub>2</sub>.

# Total Carbon Storage, Change from Contemporary

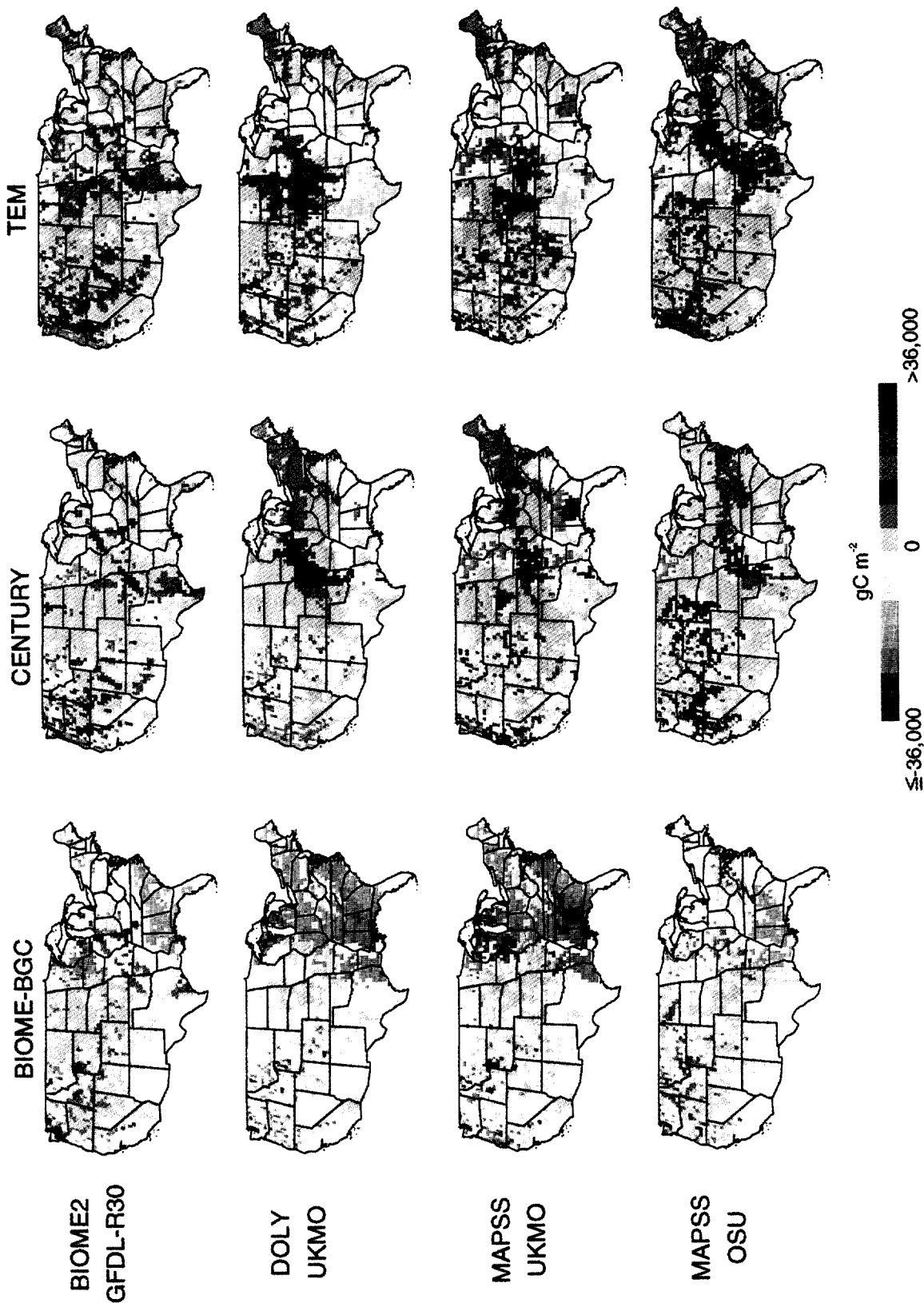


**Plate 6.** Comparison of changes in carbon stored in both vegetation and soils (total C) as estimated when biogeochemistry models (BIOME-BGC, CENTURY, TEM) are run with the vegetation distributions of the biogeography models for particular climate scenarios (GFDL-R30, UKMO, OSU).

given class of model (e.g., biogeochemistry model) a modular structure would make it possible to exchange modules describing key ecological processes such as photosynthesis among models. By doing this we could pinpoint the conceptual differences among models and we could explore the system-level consequences of these differences. The modular approach would also improve our ability to pair models from different classes. In the present VEMAP activity, for example, the pairing of MAPSS with TEM presents a conceptual problem. In response to climate change the predicted vegetation distribution by MAPSS reflects a high sensitivity to water stress, while the predicted biogeochemistry by TEM reflects a low sensitivity to water stress. Clearly, the ideal coupling of these models would involve a common hydrologic module.

### Reduction of Uncertainties Regarding Key Processes

The VEMAP study shows that while both classes of models present rather consistent simulations of current conditions, their predictions diverge substantially when climate and CO<sub>2</sub> are altered. The differences in model predictions illustrate the consequences of the conceptual and mathematical formulations employed, and provide a quantitative view of the consequences of the various assumptions employed. While all six models employ formulations that have passed the scrutiny of publication, and can reproduce aspects of the current state, they illustrate clearly areas where the current state-of-the-science is inadequate. Key areas of divergence between the models arise from the formulation of the effects of CO<sub>2</sub> on water and nutrient use, on allocation of NPP to different plant components (explicitly or implicitly), and on long-term coupling of carbon and nitrogen storage. The models also differ in the degree to which canopy processes are coupled to the atmosphere and the feedbacks which result from this coupling. It is crucial that modelers and experimentalists communicate new results suggesting mechanisms not included in extant models.

### Validation of Models

One way to begin to narrow the range of possible responses and to determine which models are most accurate is to collect appropriate measurements from natural ecosystems that can confirm or validate the projections of the models. Certain measurements can and should be made in the near future. In particular, these include flux measurements of carbon and water exchange over large areas of major ecosystem types. Measurements over the seasonal cycle and, periodically, over several years to determine fluxes during years with different temperatures and precipitation amounts are essential. These data can be used to determine whether measured ET and net carbon exchange are consistent with values predicted by particular models. It is also important to recognize that the ability of a model to simulate current ecological conditions does not validate its ability to accurately simulate responses to future climate change. Model sensitivity to different climates may be examined by simulating ecological responses to Holocene climates or more distant past warm periods for which paleoecological data exist.

### Development of Models of Transient Ecological Responses

As explained previously, an important limitation of the VEMAP exercise is that the models only made projections about steady state or equilibrium conditions. From both a scientific and policy perspective it is critical that we develop models that incorporate transient dynamics and make real time predictions about the patterns of ecological change. This is not a trivial task, in part because of the numerous aspects of ecological response (e.g., vegetation dieback, migration, succession, soil development) that must be incorporated and because the time constants for different responses can vary widely. Several modeling groups are working on transient models, and we simply want to convey to others the critical importance of this work.

Simulations from GCMs indicate that substantial uncertainty remains with respect to the magnitude of future global warming and particularly regional climate changes. The VEMAP results indicate that uncertainty also exists in our ability to simulate ecological responses to elevated CO<sub>2</sub> and global warming. Various combinations of vegetation redistribution and altered biogeochemical cycles could produce scenarios ranging from increases in forest area and carbon sequestration to losses of forest area and losses of carbon stores. Likewise, the areas of arid regions of the United States could remain similar to today, or expand considerably. Between forest and arid regions lie grasslands and shrub-steppe regions, which exhibit complex responses. One thing seems certain from these analyses. Long-term change in ecosystem structure and function is likely, at least as likely as a continuing "status quo."

**Acknowledgments.** This study was funded by the Electric Power Research Institute, the National Aeronautics and Space Administration, and the U.S. Department of Agriculture Forest Service. We also acknowledge the National Science Foundation support of the Climate System Modeling Program of the University Corporation for Atmospheric Research. VEMAP is a research project of the Global Change in Terrestrial Ecosystems (GCTE) core project of the International Geosphere-Biosphere Programme (IGBP). The National Center for Atmospheric Research is sponsored by the National Science Foundation.

### References

- Black, J. N., C. W. Bonython, and J. A. Prescott, Solar radiation and the duration of sunshine, *Q. J. R. Meteorol. Soc.*, 80, 231-235, 1954.
- Borchers, J. R., The climate of the central North American grassland, *Ann. Assoc. Am. Geogr.*, 40, 1-39, 1950.
- Bristow, K. L., and G. S. Campbell, On the relationship between incoming solar radiation and daily maximum and minimum temperature, *Agric. For. Meteorol.*, 31, 159-166, 1984.
- Charlson, R. J., and T. M. L. Wigley, Sulfate aerosol and climatic change, *Sci. Am.*, 270, 48-57, 1994.
- Daly, C., R. P. Neilson, and D. L. Phillips, A statistical-topographic model for mapping climatological precipitation over mountainous terrain, *J. Appl. Meteorol.*, 33, 140-158, 1994.
- Daubenmire, R., Ecology of fire in grasslands, *Adv. Ecol. Res.*, 5, 209-266, 1968.
- Dirmeyer, P. A., Vegetation stress as a feedback mechanism in midlatitude drought, *J. Clim.*, 7, 1463-1483, 1994.
- Eddy, A., Interpolated Daily Surface Data: 1881-1985, Oklahoma Climatological Survey, NCAR dataset DS508.0, 1987.
- Elliott, D. L., C. G. Holladay, W. R. Barchet, H. P. Foote, and W. F. Sandusky, *Wind Energy Resource Atlas*, 210 pp., Solar Technical

- Information Program, U.S. Department of Energy, Washington, D. C. 1986.
- Farquhar, G. D., S. von Caemmerer, and J. A. Berry, A biochemical model of photosynthetic CO<sub>2</sub> assimilation in leaves of C<sub>3</sub> species, *Planta*, 149, 78-90, 1980.
- Field, C., and H. A. Mooney, The photosynthesis-nitrogen relationship in wild plants, in *On the Economy of Plant Form and Function*, edited by T. J. Givinish, 717 pp., Cambridge University Press, New York, 1986.
- Gates, D. M., *Biophysical Ecology*, Springer-Verlag, New York, 1981.
- Gates, D. M., Global biospheric response to increasing atmospheric carbon dioxide concentration, in *Direct Effects of Increasing Carbon Dioxide on Vegetation*, edited by B. R. Strain and J. D. Cure, pp. 171-184, Rep. DOE/ER-0238, U. S. Department of Energy, Washington, D. C., 1985.
- Glassy, J. M., and S. W. Running, Validating diurnal climatology logic of the MT-CLIM model across a climatic gradient in Oregon, *Ecol. Appl.*, 4, 248-257, 1994.
- Haxeltine, A., I. C. Prentice, and I. D. Cresswell, A coupled carbon and water flux model to predict vegetation structure, *J. Veg. Sci.*, in press, 1995.
- Haxeltine, A., and I. C. Prentice, A general model for the light-use efficiency of primary production, *Funct. Ecol.*, in press, 1995.
- Holland, E. A., W. J. Parton, J. K. Delting, and D. L. Coppock, Physiological response of plant population to herbivory and their consequences for ecosystem nutrient flow, *Am. Nat.*, 140(4), 685-706, 1992.
- Hunt, E. R. Jr., F. C. Martin, and S. W. Running, Simulating the effect of climatic variation on stem carbon accumulation of a ponderosa pine stand: Comparison with annual growth increment data, *Tree Physiol.*, 9, 161-172, 1991.
- Hunt, E. R. Jr., and S. W. Running, Simulated dry matter yields for aspen and spruce stands in the North American Boreal Forest, *Can. J. Remote Sens.*, 18, 126-133, 1992.
- Intergovernmental Panel on Climate Change (IPCC), *Climatic Change 1992. The Supplementary Report to the IPCC Scientific Assessment*, edited by Houghton, J. T., B. A. Callander, and S. K. Varney, Cambridge University Press, New York, 1992.
- Jarvis, P. G., and K. G. McNaughton, Stomatal control of transpiration: Scaling up from leaf to region, *Adv. Ecol. Res.*, 15, 1-49, 1986.
- Jenne, R. L., Climate model description and impact on terrestrial climate, in *Global Climate Change: Implications, Challenges and Mitigation Measures*, edited by S. K. Majumdar, L. S. Kalkstein, B. Yarnal, E. W. Miller, and L. M. Rosenfeld, 566 pp., Pennsylvania Academy of Science, Philadelphia, 1992.
- Jensen, M. E., and H. R. Haise, Estimating evapotranspiration from solar radiation. *J. Irrig. Drain. Div. Am. Soc. Civ. Eng.*, 89(IR4), 15-41, 1963.
- Kern, J. S., Spatial patterns of soil organic carbon in the contiguous United States, *Soil Sci. Soc. Am. J.*, 58, 439-455, 1994.
- Kern, J. S., Geographic patterns of soil water-holding capacity in the contiguous United States, *Soil Sci. Soc. Am. J.*, 59, 1126-1133, 1995.
- Kimball, B. A., Carbon dioxide and agricultural yield: An assemblage and analysis of 430 prior observations, *Agron. J.*, 75, 779-788, 1975.
- Kittel, T. G. F., N. A. Rosenbloom, T. H. Painter, D. S. Schimel, and VEMAP Modeling Participants, The VEMAP integrated database for modeling United States ecosystem/vegetation sensitivity to climate change. *J. Biogeography*, 22, in press, 1995a.
- Kittel, T. G. F., D. S. Ojima, D. S. Schimel, R. McKeown, J. G. Bromberg, T. H. Painter, N. A. Rosenbloom, W. J. Parton, and F. Giorgi, Model-GIS integration and dataset development for assessing the vulnerability of terrestrial ecosystems to climate change, in *Proceedings Volume, NCGIA Second International Conference on Integrating GIS and Environmental Modeling*, GIS World Books, Ft. Collins, Colo., in press, 1995b.
- Knight, D. H., T. J. Fahey, and S. W. Running, Factors affecting water and nutrient outflow from lodgepole pine forests in Wyoming, *Ecol. Monogr.*, 55, 29-48, 1985.
- Korol, R. L., S. W. Running, K. S. Milner, and E. R. Hunt Jr., Testing a mechanistic carbon balance model against observed tree growth, *Can. J. For. Res.*, 21, 1098-1105, 1991.
- Küchler, A. W., Potential Natural Vegetation of the Conterminous United States, manual to accompany the map, Spec. Publ. 36, 143 pp., Am. Geogr. Soc., New York, 1964.
- Küchler, A. W., Potential Natural Vegetation of the United States, 2nd ed., map 1:3,168,000, Am. Geogr. Soc., New York, 1975.
- Leuning, R., Modelling stomatal behavior and photosynthesis of *Eucalyptus grandis*, *Aust. J. Plant Physiol.*, 17, 159-175, 1990.
- Linacre, E. T., Estimating the net radiation flux, *Agric. Meteorol.*, 5, 49-63, 1968.
- Manabe, S., R. T. Wetherald, J. F. B. Mitchell, V. Meleshko, and T. Tokioka, Equilibrium Climate Change--and its Implications for the Future, in *Climate Change: The IPCC Scientific Assessment*, edited by J. T. Houghton, G. J. Jenkins, and J. J. Ephraums, pp. 131-172, Cambridge University Press, New York, 1990.
- Marks, D., The sensitivity of potential evapotranspiration to climate change over the continental United States, in *Biospheric Feedbacks to Climate Change: The Sensitivity of Regional Trace Gas Emissions, Evapotranspiration, and Energy Balance to Vegetation Redistribution*, edited by H. Gucinski, D. Marks, and D. P. Turner, pp. IV-1 - IV-31, EPA/600/3-90/078, U. S. Environmental Protection Agency, Corvallis, Oreg., 1990.
- Marks, D., and J. Dozier, Climate and energy exchange at the snow surface in the alpine region of the Sierra Nevada, 2, Snow cover energy balance, *Water Resour. Res.*, 28, 3043-3054, 1992.
- McGuire, A. D., J. M. Melillo, L. A. Joyce, D. W. Kicklighter, A. L. Grace, B. Moore III, and C. J. Vörösmarty, Interactions between carbon and nitrogen dynamics in estimating net primary productivity for potential vegetation in North America, *Global Biogeochem. Cycles*, 6, 101-124, 1992.
- McGuire, A. D., L. A. Joyce, D. W. Kicklighter, J. M. Melillo, G. Esser, and C. J. Vörösmarty, Productivity response of climax temperate forests to elevated temperature and carbon dioxide: A North American comparison between two global models, *Clim. Change*, 24, 287-310, 1993.
- McGuire, A. D., J. M. Melillo, D. W. Kicklighter, and L. A. Joyce, Equilibrium responses of soil carbon to climate change: Empirical and process-based estimates, *J. Biogeography* 22, in press, 1995a.
- McGuire, A. D., D. W. Kicklighter, and J. M. Melillo, Global climate change and carbon cycling in grasslands and conifer forests, in *Global Change: Effects on Coniferous Forests and Grasslands*, edited by J. M. Melillo, and A. I. Breymeyer, SCOPE volume chapter, in press, 1995b.
- McLeod, S., and S. W. Running, Comparing site quality indices and productivity of ponderosa pine stands in western Montana, *Can. J. For. Res.*, 18, 346-352, 1988.
- Meentemeyer, V., The geography of organic decomposition rates, *Ann. Assoc. Am. Geogr.*, 74, 511-560, 1984.
- Melillo, J. M., T. V. Callaghan, F. I. Woodward, E. Salati, and S. K. Sinha, Climate change-effects on ecosystems, in *Climatic Change: The IPCC Scientific Assessment*, edited by J. T. Houghton, G. J. Jenkins, and J. J. Ephraums, pp. 282-310, Cambridge University Press, New York, 1990.
- Melillo, J. M., A. D. McGuire, D. W. Kicklighter, B. Moore III, C. J. Vörösmarty, and A. L. Schloss, Global climate change and terrestrial net primary production, *Nature*, 363, 234-240, 1993.
- Melillo, J. M., D. W. Kicklighter, A. D. McGuire, W. T. Peterjohn, and K. M. Newkirk, Global change and its effects on soil organic carbon stocks, *Role of Nonliving Organic Matter in the Earth's Carbon Cycle*, edited by R. G. Zepp and Ch. Sontagg, pp. 175-189, John Wiley, New York, 1995.
- Metherell, A. K., Simulation of soil organic matter dynamics and nutrient cycling in agroecosystems, Ph.D. Dissertation, Colorado State University, Fort Collins, 1992.
- Monserud, R. A., and R. Leemans, Comparing global vegetation maps with the Kappa statistic, *Ecol. Model.*, 62, 275-293, 1992.
- Monteith, J. L., Evaporation and surface temperature, *Q. J. R. Meteorol. Soc.*, 107, 1-27, 1981.
- National Climatic Data Center (NCDC), 1961-1990 Monthly Station Normals Tape, U. S. Department of Commerce, data tape TD 9641, 1992.
- Neilson, R. P., A model for predicting continental-scale vegetation distribution and water balance, *Ecol. Appl.* 5, 362-385, 1995.
- Neilson, R. P., and D. Marks, A global perspective of regional vegetation and hydrologic sensitivities from climate change, *J. Veg. Sci.* 5, 715-730, 1995.
- Neilson, R. P., G. A. King, and G. Koerper, Toward a rule-based biome model, *Landscape Ecol.*, 7, 27-43, 1992.

- Nemani, R. R., and S. W. Running, Testing a theoretical climate-soil-leaf area hydrologic equilibrium of forests using satellite data and ecosystem simulation, *Agric. For. Meteorol.*, **44**, 245-260, 1989.
- Nobre, C. A., P. J. Sellers, and J. Shukla, Amazonian deforestation and regional climatic change, *J. Clim.*, **4**, 957-988, 1991.
- Ojima, D. S., W. J. Parton, D. S. Schimel, and C. E. Owensby, Simulated impacts of annual burning on prairie ecosystems, in *Fire in North American Tallgrass Prairies*, edited by S. L. Collins and L. L. Wallace, 175 pp., Univ. of Oklahoma Press, Norman, Okla. and London, England, 1990.
- Parton, W. J., D. S. Schimel, C. V. Cole, and D. S. Ojima, Analysis of factors controlling soil organic matter levels in Great Plains grasslands, *Soil Sci. Soc. Am. J.*, **51**, 1173-1179, 1987.
- Parton, W. J., J. W. B. Stewart, and C. V. Cole, Dynamics of C, N, P and S in grassland soils: A model, *Biogeochemistry*, **5**, 109-131, 1988.
- Parton, W. J., et al., Observations and modeling of biomass and soil organic matter dynamics for the grassland biome worldwide, *Global Biogeochem. Cycles*, **7**(4), 785-809, 1993.
- Penner, J. E., C. S. Atherton, and T. E. Graedel, Global emissions and models of photochemically active compounds, in *Global Atmospheric-Biospheric Chemistry*, edited by R. Prinn, pp. 223-247, Plenum, New York, 1994.
- Pierce, L. L., Scaling ecosystem models from watersheds to regions: Tradeoffs between model complexity and accuracy, Ph.D. dissertation, 146 p., School of Forestry, Univ. of Montana, 1993.
- Prentice, I. C., and I. Fung, The sensitivity of terrestrial carbon storage to climate change, *Nature*, **346**, 48-51, 1990.
- Prentice, I. C., W. Cramer, S. P. Harrison, R. Leemans, R. A. Monserud, and A. M. Solomon, A global biome model based on plant physiology and dominance, soil properties and climate, *J. Biogeogr.*, **19**, 117-134, 1992.
- Raich, J. W., E. B. Rastetter, J. M. Melillo, D. W. Kicklighter, P. A. Steudler, B. J. Peterson, A. L. Grace, B. Moore III, and C. J. Vörösmarty, Potential net primary productivity in South America: Application of a global model, *Ecol. Appl.*, **1**, 399-429, 1991.
- Rastetter, E. B., A. W. King, B. J. Crosby, G. M. Hornberger, R. V. O'Neill, and J. E. Hobbie, Aggregating fine-scale ecological knowledge to model coarser-scale attributes of ecosystems, *Ecol. Appl.*, **2**, 55-70, 1992.
- Richardson, C. W., Stochastic simulation of daily precipitation, temperature and solar radiation, *Water Resour. Res.*, **17**(1), 182-190, 1981.
- Richardson, C. W., and D. A. Wright, WGEN: A Model for Generating Daily Weather Variables, *Rep. ARS-8*, 83 pp., U. S. Dep. of Agric., Agric. Res. Ser., reproduced by National Technical Information Service, U. S. Dep. of Commerce, Springfield, VA, 22161, 1984.
- Rizzo, B., and E. Wiken, Assessing the sensitivity of Canada's ecosystems to climatic change, *Clim. Change*, **20**, 81-95, 1992.
- Running, S. W., Testing FOREST-BGC ecosystem process simulations across a climatic gradient in Oregon, *Ecol. Appl.*, **4**, 238-247, 1994.
- Running, S. W., and J. C. Coughlan, A general model of forest ecosystem processes for regional applications, I, Hydrologic balance, canopy gas exchange and primary production processes, *Ecol. Model.*, **42**, 125-154, 1988.
- Running, S. W., and S. T. Gower, FOREST-BGC, a general model of forest ecosystem processes for regional applications, II, Dynamic carbon allocation and nitrogen budgets, *Tree Physiol.*, **9**, 147-160, 1991.
- Running, S. W., and E. R. Hunt Jr., Generalization of a forest ecosystem process model for other biomes, BIOME-BGC, and an application for global-scale models, in *Scaling Processes Between Leaf and Landscape Levels*, edited by J. R. Ehleringer, and C. Field, pp. 141-158, Academic, San Diego, Calif., 1993.
- Running, S. W., R. R. Nemani, and R. D. Hungerford, Extrapolation of synoptic meteorological data in mountainous terrain and its use for simulating forest evapotranspiration and photosynthesis, *Can. J. For. Res.*, **17**, 472-483, 1987.
- Running, S. W., T. R. Loveland, and L. L. Pierce, A vegetation classification logic based on remote sensing for use in global biogeochemical models, *Ambio*, **23**(1), 77-81, 1994.
- Sanford, R. L. Jr., W. J. Parton, D. S. Ojima, and D. J. Lodge, Hurricane effects on soil organic matter dynamics and forest production in the Luquillo Experimental Forest, Puerto Rico: Results of simulation modeling, *Biotropica*, **23**(4a), 364-372, 1991.
- Schimel, D. S., B. H. Braswell, E. A. Holland, R. McKeown, D. S. Ojima, T. H. Painter, W. J. Parton, and A. R. Townsend, Climatic, edaphic, and biotic controls over storage and turnover of carbon in soils, *Global Biogeochem. Cycles*, **8**, 279-293, 1994.
- Schlesinger, M. E., and Z.-C. Zhao, Seasonal climate changes induced by doubled CO<sub>2</sub> as simulated by the OSU atmospheric GCM-mixed layer ocean model, *J. Clim.*, **2**, 459-495, 1989.
- Shea, D. J., The Annual Cycle, I, The Annual Variation of Surface Temperature over the United States and Canada, *NCAR Tech. Note, NCARTN-242+STR*, p. 77, Natl. Cent. for Atmos. Res., Boulder Colo., 1984.
- Trenberth, K. E., G. W. Branstator, and P. A. Arkin, Origins of the 1988 North American drought, *Science*, **242**, 1640-1645, 1988.
- Vitousek, P. M., T. Fahey, D. W. Johnson, and M. J. Swift, Element interactions in forest ecosystems: Succession, allometry, and input-output budgets, *Biogeochemistry*, **5**, 7-34, 1988.
- Vörösmarty, C. J., B. Moore III, A. L. Grace, M. P. Gildea, J. M. Melillo, B. J. Peterson, E. B. Rastetter, and P. A. Steudler, Continental scale models of water balance and fluvial transport: An application to South America, *Global Biogeochem. Cycles*, **3**, 241-265, 1989.
- Walker, B. H., Landscape to regional-scale responses of terrestrial ecosystems to global change, *Ambio*, **23**, 67-73, 1994.
- Wetherald, R. T., S. Manabe, U. Cubasch, and R. D. Cess, Processes and Modelling in *Climate Change: The IPCC Scientific Assessment*, edited by J. T. Houghton, G. J. Jenkins, and J. J. Ephraums, pp. 69-91, Cambridge University Press, New York, 1990.
- White, J. D., and S. W. Running, Testing scale dependent assumptions in regional ecosystem simulations, *J. Veg. Sci.*, **5**, 687-702, 1995.
- Wilson, C. A., and J. F. B. Mitchell, A doubled CO<sub>2</sub> climate sensitivity experiment with a global climate model including a simple ocean, *J. Geophys. Res.*, **92**(D11), 13,315-13,343, 1987.
- Woodrow, I. E., and J. A. Berry, Enzymatic regulation of photosynthetic CO<sub>2</sub> fixation in C<sub>3</sub> plants, *Annu. Rev. Plant Physiol.*, **39**, 533-594, 1988.
- Woodward, F. I., and T. M. Smith, Predictions and measurements of the maximum photosynthetic rate at the global scale, in *Ecophysiology of Photosynthesis*, edited by E.-D. Schulze, and M. M. Caldwell, pp. 491-509, *Ecological Studies*, vol. 100, Springer-Verlag, New York, 1994a.
- Woodward, F. I., and T. M. Smith, Global photosynthesis and stomatal conductance: Modelling the controls by soil and climate, *Bot. Res.*, **20**, 1-41, 1994b.
- Woodward, F. I., T. M. Smith, and W. R. Emanuel, A global land primary productivity and phytogeography model, *Global Biogeochem. Cycles*, in press, 1995.
- J. Borchers, J. Chaney, and R. Neilson, U.S. Department of Agriculture Forest Service, Oregon State University, Forest Science Laboratory, 3200 S.W. Jefferson Way, Corvallis, OR 97333 (e-mail: borchers@fsl.orst.edu; jchaney@fsl.orst.edu; neilson@fsl.orst.edu)
- H. Fisher, T. G. F. Kittel, and D. S. Schimel, UCAR, P.O. Box 3000, Boulder, CO 80307-3000 (e-mail: fisherh@sage.cgd.ucar.edu; tim\_kittel@qgate.ucar.edu; schimel@sage.cgd.ucar.edu)
- S. Fox, U. S. Department of Agriculture Forest Service, 1509 Varsity Dr., Research Triangle, Raleigh NC 27606 (e-mail: susan@essnv5.rrc.ncsu.edu)
- A. Haxeltine, C. Prentice, and S. Sitch, University of Lund, östra Vallstian 14, 22361, Lund, Sweden (e-mail: alex@planteco.lu.se; colin.prentice@planteco.lu.se; Stephen.Sitch@planteco.lu.se)
- A. Janetos, National Aeronautics and Space Administration, NASA HQ Code SEP03, Washington, D.C. 20546 (e-mail: tjanetos@mtpe.hq.nasa.gov)
- D. W. Kicklighter, J. M. Melillo, and Y. Pan, The Ecosystems Center, Marine Biological Laboratory, Woods Hole, MA 02543 (e-mail: dkick@lupine.mbl.edu; jmelillo@lupine.mbl.edu; yudepan@lupine.mbl.edu)
- A. D. McGuire, Alaska Cooperative Fish and Wildlife Research Unit, 216 Irving I, University of Alaska-Fairbanks, Fairbanks, AK 99775-7020 (e-mail: FFADM@aurora.alaska.edu)
- R. McKeown, D. S. Ojima, and W. J. Parton, NREL, Colorado State

University, Fort Collins, CO 80523-1499 (e-mail: beckym@nrel.colostate.edu; dennis@poa.nrel.colostate.edu; billP@poa.nrel.colostate.edu)

R. Nemani and S. Running, University of Montana, Missoula, MN 59812 (e-mail: nemani@hps1.ntsg.umt.edu;)

T. Painter, Center for Remote Sensing and Environmental Optics, University of California, Santa Barbara, CA 93106 (e-mail: painter@crseo.ucsb.edu)

L. Pierce, Department of Biological Sciences, Stanford University, Stanford, CA 94305 (lars@jasper.stanford.edu)

L. Pitelka, EPRI, P.O. Box 10412, Palo Alto, CA 94303 (e-mail: lpitelka@msm.epri.com)

B. Rizzo and T. Smith, Department of Environmental Sciences, University of Virginia, Charlottesville, VA 22903 (e-mail: br7q@amazon.evsc.virginia.edu; tms9a@virginia.edu)

N. A. Rosenbloom, Department of Geology/INSTAAR, University of Colorado, Boulder, CO 80309 (e-mail: nanr@sage.cgd.ucar.edu)

I. Woodward, Department of Animal and Plant Sciences, University of Sheffield, P. O. Box 601, Sheffield, S10 2UQ, UK (e-mail: f.i.woodward@sheffield.ac.uk)

(Received March 13, 1995; revised September 5, 1995; accepted September 8, 1995.)

